2017

MODIFIED PAMAM DENDRIMERS IN TUNABLE DRUG-DELIVERY SYSTEMS: A SUSTAINED-RELEASE DENDRIMER HYDROGEL FOR ANTI-GLAUCOMA DRUGS AND SURFACE-ENGINEERED MACROPHAGES AS NANOPARTICLE CARRIERS FOR TARGETED ANTI-CANCER THERAPY

Christopher A. Holden
Virginia Commonwealth University

MODIFIED PAMAM DENDRIMERS IN TUNABLE DRUG-DELIVERY SYSTEMS: A SUSTAINED-RELEASE DENDRIMER HYDROGEL FOR ANTI-GLAUCOMA DRUGS AND SURFACE-ENGINEERED MACROPHAGES AS NANOPARTICLE CARRIERS FOR TARGETED ANTI-CANCER THERAPY

A thesis submitted in partial fulfillment of the requirements for the degree of Master of Science in Biomedical Engineering at Virginia Commonwealth University

by

CHRISTOPHER ALAN HOLDEN

Bachelor of Science, University of Virginia, 2007

Director: Hu Yang, Ph.D., Professor, Chemical and Life Science Engineering

Co-chair: Rebecca Heise, Ph.D., Associate Professor, Biomedical Engineering

Virginia Commonwealth University

Richmond, Virginia

August 7, 2017

Acknowledgements

First and foremost, I would like to thank my adviser Dr. Yang and his lab for the support in my long journey of finishing my thesis. His lab pushed me to move outside of my comfort zone to learn new skills and delve into new projects. I have grown and learned a great deal about organic chemistry techniques and syntheses from my experiences in his lab. I would also like to thank Dr. Andrew Yeudall for his guidance and support in his lab at the VCU School of Dentistry; I gained valuable experience with biological assays from working with him and his students. Thanks goes to my co-chair Dr. Rebecca Heise and also to Dr. Daniel Conway for taking the time to work on my committee. Another thanks goes to Dr. Jennifer Wayne for her help along the way as Graduate Program Director.

I would also like to thank my friends and family for their constant love and support in my academic, personal, and professional life. Specifically, I would like to thank my friend Caro who has helped me over some of my toughest hurdles; she continually encouraged me to push forward to achieve my goals.

This research was supported in part by The Jeffress Memorial Trust (J-873), the National Institutes of Health (R21NS063200), and the Wallace H. Coulter foundations.

Table of Contents

List of Tables

List of Figures

Abstract

MODIFIED PAMAM DENDRIMERS IN TUNABLE DRUG-DELIVERY SYSTEMS: A SUSTAINED-RELEASE DENDRIMER HYDROGEL FOR ANTI-GLAUCOMA DRUGS AND SURFACE-ENGINEERED MACROPHAGES AS NANOPARTICLE CARRIERS FOR TARGETED ANTI-CANCER THERAPY

By Christopher Alan Holden, B.S.

A thesis submitted in partial fulfillment of the requirements for the degree of Master of Science in Biomedical Engineering at Virginia Commonwealth University

Virginia Commonwealth University, 2017

Director: Hu Yang, Ph.D., Professor, Chemical and Life Science Engineering

Co-chair: Rebecca Heise, Ph.D., Associate Professor, Biomedical Engineering

Two specific drug-delivery applications were sought in this work using polyamidoamine (PAMAM) dendrimers. One drug-delivery system used a novel dendrimer hydrogel (DH) for sustained delivery of anti-glaucoma drugs. In this work, PAMAM G3.0 dendrimers were covalently bonded with poly(ethylene glycol) (PEG_{12000}) molecules which were subsequently acrylated, resulting in photocurable DH conjugates. For pharmacological studies, DH were loaded with a solution of intraocular pressure lowering drugs, brimonidine and timolol maleate,

and were characterized for *in vitro* release and *ex vivo* transport and uptake. DH formulations were shown to increase the loading of drug molecules, increase transcorneal drug delivery, and exhibit sustained-delivery of drug molecules. A second drug-delivery system, utilizing cell-surface engineering, intended to increase the targeting ability of highly toxic anti-cancer drugs to curtail systemic effects. In particular, Qdots and 5-(aminoacetamido) fluorescein-labeled polyamidoamine dendrimer G4.5, both of which were coated with amine-derivatized polyethylene glycol, were immobilized to the sodium periodate-treated surface of RAW264.7 macrophages through a transient Schiff base linkage. Further, a reducing agent sodium cyanoborohydride was applied to reduce Schiff bases to stable secondary amine linkages. The distribution of nanoparticles on the cell surface was observed by fluorescence microscopy and was found to be dependent on the stability of the linkages tethering nanoparticles to the cell surface.

Chapter 1 Introduction

Exciting frontiers in pharmaceutical science research arise from limitations in the innate kinetics of drug molecules. Drug molecules have unique profiles in their distribution, uptake, absorption, and clearance within the body. These pharmacokinetic properties are typically dependent on route of administration(ROA) and formulation. Each ROA has different sets of pros and cons depending on the class of drug molecules and the clinical target. The goal in drug delivery is to maximize the efficiency of a drug formulation to reach the therapeutic window of drug molecules within the body. Drug delivery strategies rely not only on the concentration and frequency of dosing, but also on the vehicle of the drug formulation. Traditional clinical strategies include, but are not limited to, drugs in solid or liquid form administered intravenously, orally, nasally, rectally, topically, or subcutaneously. Therapeutic efficacy is based on the innate pharmacokinetics; yet, by using biomaterial research and cellular therapies the efficacy of drugs can be enhanced. This project utilizes biomaterial nanoparticle vehicles to enhance drug molecules and treatment options.

Biomaterial research has led to advances in wound healing, tissue engineering, and drug delivery. Natural and synthetic classes of biomaterials are used either independently or in conjunction with other materials and biologics for desired applications. In this work polyamidoamine (PAMAM) dendrimers, a class of synthetic polymeric nanoparticles, are explored for their versatile physical and chemical properties. Dendrimers are a highly organized polymer branching from an ethylene diamine core structure that are stepwise synthesized to create amine terminated (full generation [X.0]) and carboxyl terminated (half generation [X.5])

nanoparticle. The amine and carboxyl functional groups allow for a highly tunable molecule using organic chemistry conjugations. This work employs PAMAM dendrimers as a key component in biomaterial drug-delivery systems including a topical hydrogel system for sustained ocular delivery as well as proof of concept for targeted drug delivery using a cellular vehicle hybridized with dendrimers.

1.1 Anti-glaucoma drug delivery

Vision, as one of the main sensory inputs, is critical in many aspects of everyday life. Visual-impairment can have a huge impact on quality of life, healthcare costs, and socioeconomic outcomes. Some of the major causes of visual-field loss are cataracts, age-related macular degeneration, diabetic retinopathy, retinal vein-occlusive diseases, and glaucoma. Specifically, glaucoma affects 2.7 million people in the United States alone(1). Currently there are no cures for glaucoma, but there are effective drug molecules for treating the causes of vision-loss in glaucoma patients. The typical treatment for glaucoma are topical eye-drop solutions administered multiple times daily; however, this tedious regimen often decreases patient compliance which leads to chronic and progressive neurodegeneration of the optic nerve. A major goal in anti-glaucoma drug delivery is to decrease the frequency of dosing to increase patient compliance and outcomes. This project proposes a topical dendrimer hydrogel co-drug formulation as a sustained delivery approach for treatment.

1.2 Targeted dendrimer delivery with cellular therapy

Many traditional cancer therapies use highly toxic drugs administered at systemic doses. Drug targeting is desired to decrease the harmful effects of chemotherapeutics on healthy cells. This project proposes an interdisciplinary approach which utilizes tools from cell biology to integrate biomaterial engineering with cancer research. Monocytes have an inherent ability to

infiltrate tumors based on factors such as hypoxia and chemoattractants. The overall goal is to utilize monocyte-targeting to deliver cancer therapies. This project sought to demonstrate that surface modification of monocytes is possible to allow hybridization with a drug-loaded biomaterial, specifically half-generation PAMAM dendrimer conjugates (PAMAM G4.5). A molecular approach through cell-surface modification of sialic acid residues on monocytes is explored. Sodium periodate modifies sialic acid into aldehyde groups which are reactive to the amines of G4.5-PEG-NH_2 conjugates through transient Schiff linkages. A stabilizing reagent, sodium cyanoborohydride, is used to reduce the linkage to a stable amide bond. In review, this thesis covers the synthesis and characterization of two drug delivery systems and demonstrates *in vitro* and *ex vivo* testing to substantiate further work using these novel approaches.

Chapter 2 Background and Significance

2.1.1 Glaucoma

According to a 2014 World Health Organization fact sheet, 285 million people worldwide suffer from visual impairment, where up to 80% of incidences are preventable or curable. Unoperated-upon cataracts and uncorrected refractive errors account for 76% of all cases of visual-impairment, but with treatment visual-field loss is reversible(2). Glaucoma, on the other hand, is the number one cause of irreversible blindness in the world(3). With early treatment, however, optic nerve damage and visual-impairment can be reduced or prevented. It is estimated that currently 60 million people suffer from glaucoma and by 2040 it is projected 112 million people will have glaucoma(4, 5). There is a clear clinical need to reduce the negative effects of the disease which include a lower quality of life and higher economic burden for those experiencing vision-loss.

Glaucoma describes a group of neuropathies which cause a progressive degeneration of retinal ganglion cells, cupping of the optic disc, and thinning of retinal nerve fibers(6). The two main classifications of glaucoma are open-angle and angle closure. In open-angle glaucoma, there is an opening between the iris and cornea, but the aqueous humor outflow is restricted through the trabecular meshwork. In angle-closure glaucoma, the drain between iris and cornea is closed and outflow through the trabecular meshwork is blocked. Currently there is no treatment for reversing nerve damage in glaucoma patients, so treating the main risk factor of increased intraocular pressure (IOP) is the primary clinical goal. IOP is a dynamic balance of fluid secreted by the ciliary body into the aqueous humor and drainage of aqueous humor. The

main treatment options include topical instillation of eye drops, which typically target either a decreased production of aqueous humor or increased aqueous humor outflow. The main clinical IOP-lowering drug classes are described below(7).

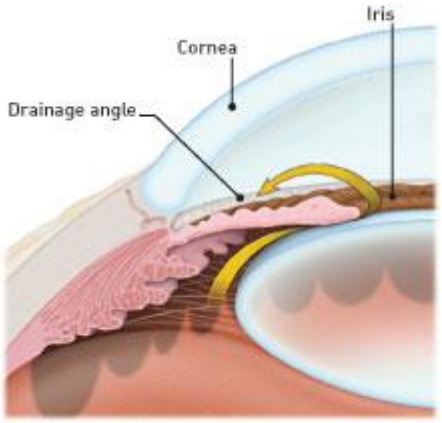

Figure 2.1 Depiction of aqueous humor outflow adapted from https://www.aao.org/eye-health/diseases/glaucoma-causes

2.1.2 IOP-lowering therapies

There are 5 major classes of drugs for lowering IOP in patients; Cholinergic agents, prostaglandin receptor analogues, β-blockers, α-adrenergic agonists, and carbonic anhydrase inhibitors. Cholinergic agents act on muscarinic receptors on ciliary muscle to increase outflow via trabecular meshwork. An example is pilocarpine, which often uses a 4 times daily dosing strategy with side effects including myopia, miosis of the pupil, and dimming of vision(7).

Prostaglandin F receptor(PTGFR) analogues with a once daily dosing increase aqueous humor outflow by altering ECM in the ciliary muscle/trabecular meshwork. Side effects of PTGFR analogues include lengthening of eyelashes, thickening of eyelashes, and darkening of the iris(7).

β-adrenergic receptor blockers have an increased tolerability and increased IOP-lowering efficacy. β -blocker treatments inhibit β-adrenergic receptors in the ciliary epithelium and help to decrease aqueous humor formation. Side effects of timolol maleate at higher dosing frequencies include syncope, arrhythmia, and dyspnea. It is thought that decreases in dosing will likely limit adverse systemic effects(7).

α-adrenergic agonists, such as brimonidine, lower IOP through stimulation of α2-adrenergic receptors which decreases aqueous humor in flow and increases uveoscleral outflow. Similar to β -blockers, α-adrenergic agonists only lower IOP during the day(7).

Carbonic anhydrase inhibitors are another IOP-lowering class and they decrease aqueous humor formation by inhibiting carbonic anhydrase II in the ciliary epithelium. Carbonic anhydrase inhibitors are typically second line agents and are effective day or night(7).

There are also FDA approved drug combination therapies that aim to simultaneously decrease aqueous humor inflow and increase outflow. These multi-drug formulations have multiple mechanisms of action and are more effective than single drugs at lowering IOP. The main issue of IOP lowering drugs is not necessarily the efficacy of action, but the efficiency of delivery and dosing regimen required to maintain therapeutic drug levels in patients.

2.1.3 Ocular drug delivery

Treatment of ocular diseases involves optimizing drug bioavailability in ocular tissues for a therapeutic response, where transcorneal permeation is the primary route of drug transport into the aqueous humor and conjunctival absorption is considered an alternative route of transport. Systemic drug delivery is typically not feasible for ocular drugs due to the blood-retinal and blood-aqueous barriers. The main barriers in topical ophthalmic drug delivery include corneal epithelial tight junctions, lacrimal clearance, conjunctival absorption, metabolism, and inadvertent protein binding(8). The shortfalls of eye drop formulations include quick precorneal clearance and low bioavailability of drug leading to a higher dosing frequency for patients. A high dosing frequency often leads to lower patient compliance and increased side effects. One solution to increase drug absorption into ocular tissues is to increase corneal residence time via electrostatic interactions with negatively charged cell membranes as well as binding with native

proteins such as mucin. Creating a more bioadhesive formulation would help alleviate some of the drug loss due to tearing. The main attachment targets for bioadhesion on the ocular surface are the mucous coat on the surface tissue and epithelial tissues(9).

Some ocular drug delivery formulations have used water soluble polymers, nanoparticles, liposomes, cellulose derivatives, mucus glycoproteins, and hyaluronate to increase corneal residence time through increased viscosity and bioadhesion. Likewise, in situ forming gels activated by pH or temperature have also been used to enhance transcorneal delivery. Dendrimers have been tested as ophthalmic vehicles for pilocarpine nitrate; in this work they were proposed to exhibit bioadhesiveness and increased corneal residence times. Other solutions aim to transiently increase transcorneal delivery through use of absorption promoters or penetration enhancers. Examples of penetration enhancers include calcium chelators (such as EDTA), surfactants, and micelles which disrupt epithelial tight junctions to allow increased paracellular permeation(9, 10). An ideal ocular formulation will likely combine characteristics including increased viscosity, increased precorneal residence, increased transcorneal transport, sustained delivery, and concomitant drugs.

2.1.4 Hydrogels

Physical and chemical hydrogels

Hydrogels are networks of polymers and colloids with either physical or chemical crosslinking that retain aqueous solutions. Physical hydrogels are networks held together by polymer entanglements, ionic interactions, or hydrogen bonding. Physical hydrogels can include anionic and cationic polymer combinations such as alginate and chitosan that self-entangle into gels. Polymers such as PEG-PLA, agarose, and gelatin can dissolve in water as random structures and can organize into helices upon heating or cooling processes to form rigid and

reversible sol-gels(11, 12). Chemical hydrogels have networks linked with covalent bonds and are the most frequently explored class in hydrogel research. Chemical hydrogels involve covalently crosslinking functional side chains or end groups of polymers with monomers or chemical treatments. UV and ionizing radiation are also used as crosslinking methods through free radical polymerization. Typically, physical hydrogels are weaker, more transient, and less customizable than chemical hydrogels(13).

Natural and synthetic hydrogels

Other than physical or chemical crosslinking, hydrogels can also be characterized as either having synthesized or naturally occurring components. Natural hydrogels are formed from proteins and polysaccharides including extracellular matrix proteins such as collagen and gelatin or polysaccharides such as agarose or alginate. Natural hydrogels typically exhibit better qualities of biocompatibility and biodegradation, but they are often less-customizable. Synthetic hydrogels include artificial polymers that are synthesized in labs. Artificial hydrogels are highly tunable and easily tailored to specific applications in the synthesis process. Water content, mechanical properties, chemical properties, mesh size, and polymer length can all be customized in synthetic hydrogels for specific biomedical functions(13).

Hydrogels in biomedical applications

Hydrogels show promising characteristics for controlled release of bioactive molecules and as scaffolds for cell growth. Design considerations for hydrogels include gelation conditions, biodegradation, biocompatibility, and synthesis. Hydrogels can also respond to biological conditions such as changes in temperature, pH, and ionic conditions to swell or contract; such responses by hydrogels allow exploitation of local conditions in delivery systems. Examples of

commercially available hydrogels include wound dressings, drug delivery vehicles, tissue scaffolds, contact lenses, diapers, and biosensors(13).

Dendrimer hydrogels

Dendrimer nanoparticles, with their highly branched architecture, are ideal molecules for crosslinking into hydrogel networks due to their surface functionality. Previous work with PAMAM dendrimers tested the effects of PEG length and degree of PEGylation, PEG molecules per dendrimer, in formation of photocurable hydrogels. It was demonstrated that $PEG_{12,000}$ created effective solid hydrogels after coupling with acrylate groups. Demonstrating synthesis of dendrimer hydrogels (DH) shows promise in drug delivery and tissue engineering applications. The hydrogel network is potentially a scaffold for cell growth or as a substrate for loading both hydrophobic and hydrophilic drug molecules. Recent research demonstrates PEGs with predetermined breaking points could add further control to PEGylated DHs and lead to new routes of biodegradation and sustained delivery(14, 15).

2.2 Dendrimers

Dendrimers are a class of nanoparticles with a highly organized structure resembling the branches or roots of trees. Expanding from a central core molecule, each stepwise monomer addition branches at a covalent bond to double the existing number of terminal groups. As the dendrimer expands, there is an incremental increase in molecular weight, diameter, and surface groups.

Dendrimers are favorable vehicles for drug delivery due to their surface group functionality, low polydispersity, hydrophobic cores, and globular structure. Full-generation (polycationic) and half-generation (polyanionic) dendrimers, with their amine and carboxyl terminal groups, allow for an array of organic chemistry coupling techniques. Polycationic

dendrimers have a shorter blood circulation time as electrostatic interactions with negatively charged cell walls lead to a rapid clearance whereas polyanionic dendrimers can have lower cytotoxicity and longer circulation time in the body as they are repelled by the negative surface potentials of cell walls. Individual dendrimers can be engineered for biocompatibility, drug loading, and targeting to satisfy a variety of biomedical applications. Specifically, PAMAM dendrimers tethered with poly(ethylene glycol) (PEG) chains have stealth properties, solubility in a range of solvents, and high biocompatibility as they are not readily recognized by the reticuloendothelial system. The propensity of dendrimers for drug-loading is an advantage over other systems as multiple drug molecules can be covalently bonded to surface functional groups of a single dendrimer for concentrated delivery. In addition to covalent drug loading, the hydrophobic backbone core of dendrimers can encapsulate hydrophobic drugs into the network with or without surface group loading. These unique properties allow dendrimer systems to have dual drug-loading to optimize therapeutic responses. Hybridized dendrimers have been used in polymeric micelles, hydrogels, and targeted drug-delivery with a wide range of functions. The biological properties and high modification potential of dendrimers makes them ideal building blocks for many biomedical applications. PEGylated dendrimers show low toxicity, low immunogenicity, and increased circulation time in the body and are ideal for targeted drug delivery(16-20).

2.3 Cellular Delivery of Anticancer Drugs

2.3.1 Tumor vasculature

Angiogenesis and irregular vasculature are attributes of solid tumors. Solid tumors are also associated with vascular permeability factors and poor lymphatic drainage. The irregular vasculature and permeability factors result in a leaky vasculature which allows nutrients and

oxygen to reach rapidly growing tumors; however, this leaky vasculature also facilitates an enhanced permeability of macromolecules and lipid particles into interstitial space. Once in the interstitial space, macromolecules accumulate due to the poor lymphatic drainage. These traits are known as enhanced permeability and retention (EPR). EPR can be a useful tool in treating tumors using nanoparticle and polymer conjugated chemotherapeutics(21-23). A limiting factor in using macromolecules or nanoparticles for drug delivery is the mononuclear phagocyte system(MPS). In the MPS, mononuclear cells are responsible for phagocytosing foreign particles to remove them from circulation. The addition of polyethylene glycol (PEG) to drug carriers creates stealth particles which can evade the MPS. PEGylation is a strategy which helps nanoparticle carriers to avoid phagocytosis and allows particles to accumulate in tumor tissues due to the EPR effect(23, 24).

Even if drug molecules accumulate in the extratumoral region due to EPR, there may not be sufficient distribution within tumors as many solid tumors have densely packed cells with necrotic centers. Nutrient-poor regions within tumor cores results in the formation of areas of hypoxia, establishment of chemotactic gradients, and heterogeneous microenvironments. Chemotherapeutic drugs struggle to diffuse passively into tumor cores, limiting the therapeutic response which potentially leads to drug resistances(25). Additionally, inefficient delivery necessitates the use of considerably higher drug concentrations, with resultant increased toxicity to normal cells, a major limiting factor when determining drug dosage. Thus, it is essential to develop methodology to deliver targeted-drug payloads into tumors to increase the efficacy and safety of chemotherapies. In this regard, a cellular-based delivery approach promises considerable advantages over standard drug formulations for treatment.

2.3.2 Monocyte migration

Blood monocytes play important repair roles in immune responses and are recruited into damaged or pathologic tissues in response to hypoxic or chemoattractant gradients(26). It has been demonstrated that monocytes have an innate ability to migrate to hypoxic areas, specifically, inside tumor spheroids(27). Once they are distributed into tissues, monocytes differentiate into macrophages. Basic monocyte and macrophage functions include phagocytosis of foreign particles, cytokine production, and antigen presentation. Monocytes and macrophages mediate immune and inflammatory responses and are important for recruitment of more immune cells into tissues(28). The migratory abilities of monocytes are well-documented and, when activated in response to gradients as mentioned above, could potentially act as suitable delivery vehicles for targeted therapeutics(29). Monocyte chemoattractant protein-1 (MCP-1) expression in tumors is shown to recruit monocyte-derived macrophages; studies demonstrate that an increase in MCP-1 lead to an increase in intratumoral macrophage invasion(30, 31).

2.3.4 Cellular therapies and metabolic engineering

Some chemotherapeutics, such as doxorubicin (DX), have a short plasma half-life. DX also has a wide biodistribution leading to cardiotoxicity at higher dosages(32, 33). To minimize negative effects on healthy tissues *in vivo*, drugs and nanoparticles have been conjugated with PEG to improve biocompatibity; PEGylating nanoparticles can increase plasma half-life and affect biodistribution of drugs(24). Additionally, DX has been shown to distribute poorly in hypoxic, acidic regions of tumors(34).

The proposed research aims to develop a hybrid vehicle consisting of monocytes/macrophages to which doxorubicin has been conjugated on the cell surface *via* polyamidoamine (PAMAM) dendrimer nanoparticles, to test functionality of both monocytes

and drug, and to investigate migration into and delivery of drug payload to tumor spheroids *in vitro*.

Pathways in metabolic engineering can be used to facilitate chemical modification of cells, in order to endow them with specific new or enhanced properties. Sialic acid residues are present on mammalian cell lines and can be modified by sodium periodate ($NaIO_4$) into amine-reactive aldehyde groups. The $NaIO_4$ modification allows aldehydes to couple with amines to form a transient Schiff-based linkage(35, 36). When the bond is exposed to another species, sodium cyanoborohydride (Na CBH_3), the linkage is reduced to a stabilized secondary amine bond(37). These surface techniques allow for conjugation of amine terminated and drug-loaded biomaterials on a cell exterior. The external attachment of drug molecules is helpful to protect the host cell. The use of tumor-targeting monocytes as delivery vehicles is a promising lead in drug therapy.

In this study, half generation PAMAM dendrimers with 128 carboxyl surface groups (G4.5) are used. When combined with another polymer, polyethylene glycol (PEG), these nanoparticles exhibit increased water solubility and biocompatibility(38). Administering N-hydroxysuccinimide (NHS) and 1-ethyl-3-(3-dimethylaminopropyl) carbodiimide (EDC) hydrochloride allowed COOH surface conjugation to NH_2 groups. PEG diamine are conjugated to activated PAMAM nanoparticles and leave an active NH_2 to bind to cell-surface aldehydes(39). When the degree of PEG loading is high, hydrophobic drugs can be encased at the dendrimer core(20). The avenue for immobilizing drug-loaded nanoparticles on modified cell surfaces is evident and has direct advantage over unbound drug formulations.

The overall hypothesis is that targeted delivery of chemotherapeutic drugs will enhance therapeutic response and enable the use of lower drug concentrations when applied to patients in

the future. Thus, the goal of the proposed research is to apply what is current knowledge of cancer biology, immune function, surface science, and biomaterials to create a novel, cutting edge drug delivery vehicle for cancer chemotherapeutics. This second project proposes to immobilize drug-loaded nanoparticles on the surface of monocytes for targeted tumor therapy.

Chapter 3 Polyamidoamine Dendrimer Hydrogel for Enhanced Delivery of Anti-glaucoma Drugs

The following chapter is adapted from a manuscript accepted in Nanomedicine: Nanotechnology, Biology and Medicine, July 2012, Volume 8(5), pages 776-783, DOI: https://doi.org/10.1016/j.nano.2011.08.018

3.1. Abstract

Dendrimer hydrogel (DH), made from UV-cured poly(amidoamine) PAMAM dendrimer G3.0 tethered with three polyethylene glycol (PEG, 12000 Da)-acrylate chains (8.1% w/v) in pH7.4 phosphate buffered saline (PBS), was studied for delivery of anti-glaucoma drugs—brimonidine (0.1 % w/v) and timolol maleate (0.5% w/v). DH was found to be mucoadhesive and cytocompatible with human corneal epithelial cells (HCETs). The solubility of brimonidine in DH was 77.6% higher than that in plain PBS. Both drugs were slowly released over 56-72 hours by DH *in vitro*. As compared to eye drop formulations (PBS drug solutions), DH resulted in substantially higher degrees of intracellular drug uptake by HCETs and cumulative transport across bovine cornea for both drugs as well as significantly higher adsorption of timolol maleate in corneal epithelium, stroma, and endothelium. This work demonstrated that DHs can enhance delivery of anti-glaucoma drugs in multiple aspects and represent a novel platform for ocular drug delivery.

3.2 Background

There is a high clinical demand for treating ocular diseases and priority is in increasing the delivery efficiency of therapeutic drugs to the eye. To date, safe and effective treatments of most ocular diseases rely heavily on topical applications due to ease of use and low-cost manufacturing. Conventional dosage forms including aqueous solutions, suspensions, and ointments that are administered topically and dominate the global market of ocular drug delivery, accounting for nearly 90% of marketed formulations.

To treat chronic eye diseases such as glaucoma, considerable efforts have been placed on exploring new topical drug carriers and formulations to increase ocular residence time of drugs and increase drug adsorption. Consequently, enhanced drug delivery helps extend the duration of

drug activity and reduce dosing frequency for patient compliance improvement. Non-conventional delivery systems and formulations for topical application of anti-glaucoma drugs are under rapid development. Mucoadhesive polymers such as hyaluronic acid and chitosan are able to enhance retention time and drug penetration through the corneal barriers due to their bioadhesiveness(9, 40, 41). *In situ*-forming hydrogels are liquid upon instillation and form viscoelastic gels in response to environmental changes such as pH or temperature(42-46). The application of *in situ*-forming hydrogel results in prolonged precorneal residence time and increased ocular bioavailability. In addition, since cationic liposomes can be preferentially captured at the negatively charged corneal surface, they have been investigated as carriers for delivery of ocular therapeutics(47). Nanoparticles such as PAMAM dendrimers, polyguanidilyated dendrimers, and poly(butylcyanoacrylate) nanoparticles have also been shown to improve ocular drug delivery efficiency(10, 19, 48-51).

Recently, we have developed a polyamidoamine (PAMAM) dendrimer hydrogel (DH) platform, which is made from UV-cured PAMAM dendrimer tethered with polyethylene glycol (PEG)-acrylate chains(15). By tuning concentration and its structural parameters such as the degree of PEGylation, PEG length, and acrylate density on the dendrimer, photoreactive dendrimer PEG acrylate in aqueous solutions can be partially crosslinked to form viscous solutions or completely crosslinked to form “no-flow” gel *in situ* upon exposure to UV light in the presence of an eosin Y-based photoinitiator(15). PAMAM dendrimers are highly branched nanoparticles with numerous surface groups and charges(52). Different from gels made from aliphatic polyester-ether hybrid dendritic-linear polymers reported for corneal laceration repair(53-55), the DH network allows for simultaneous delivery of both hydrophobic and hydrophilic drugs as needed. The interior hydrophobic core of the dendrimer can encapsulate

hydrophobic compounds and increase their water solubility and loading amounts(17, 56). When crosslinked, the PEG network can accommodate hydrophilic drugs. DH is likely to have excellent cytocompatibility owing to the PEG component. Furthermore, the cationic charges conferred by the DH possess unique structural characteristics and desirable properties for drug delivery. Figure 3.1 shows a representation of a drug-loaded dendrimer hydrogel.

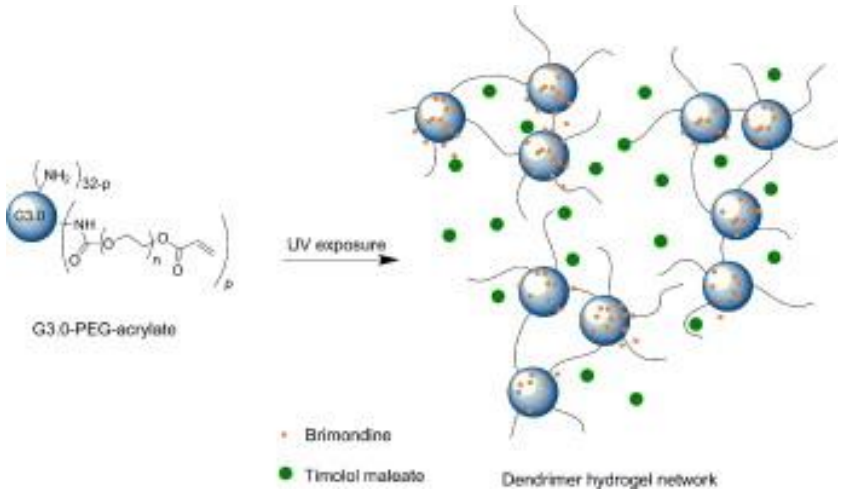

Figure 3.1 Representation of drug-loaded dendrimer hydrogel

For ocular drug delivery, the DH promises to have properties superior to dendrimer or PEG gel alone, each of which have been separately shown to be efficient as ophthalmic vehicles. Therefore, the objective of this work is to demonstrate the feasibility of utilizing DH as a topical formulation for ocular drug delivery. The anti-glaucoma drugs brimonidine and timolol maleate were used as model drugs. Mucoadhesiveness of the DH was characterized in terms of its interaction between mucin particles. Cytotoxicity of DH formulations and their ability to enhance water solubility of hydrophobic brimonidine were studied. Further, *in vitro* drug release, cellular uptake, *ex vivo* transcorneal transport, and *ex vivo* eye tissue uptake of the two drugs mediated with DH formulations were examined.

3.3 Methods and Materials

3.3.1 Synthesis of photoreactive PAMAM G3.0-PEG-acrylate conjugates

Photoreactive PAMAM G3.0-PEG-acrylate conjugates were synthesized at room temperature following our previously reported procedure with modification(15). According to Scheme 1, PEG diol (12000 $g \cdot mol^{-1}$) (1 eq.) dissolved in tetrahydrofuran (THF) was reacted with acryloyl chloride (1 eq.) first in the presence of triethylamine (TEA) (1 eq.). After overnight reaction while stirring, the salt was removed by centrifugation. The resultant OH-PEG-acrylate in the supernatant was further reacted with 4-nitrophenyl chloroformate (NPC) (1 eq.) and TEA (1 eq.). The reaction proceeded overnight while stirring. Upon the centrifugal removal of the salt, the resultant NPC-PEG-acrylate was dried through rotary evaporation. NPC-PEG-acrylate was then coupled to PAMAM dendrimer G3.0 in dimethylformamide. After 24 h reaction, G3.0-PEG-acrylate conjugates were precipitated in cold ether, dialyzed against deionized water, and freeze-dried. The conjugates were characterized with ^{1}H-NMR spectroscopy(15, 38, 56). G3.0 coupled with an average of 3 PEG acrylate chains (MW=~43,000 g mol^{-1}) was obtained and used to prepare anti-glaucoma drug formulations. FI-IR spectra were obtained from solution cast films on KBr discs using a Nicolet Magna IR 760 spectrometer.

3.3.2 Preparation of anti-glaucoma drug formulations

To prepare combination drug formulations based on DH, 40.5 mg of G3.0-PEG-acrylate was first dissolved in 500 µL of pH 7.4 phosphate buffered saline (PBS) to have a final concentration of 8.1% (w/v) in PBS. Afterwards, 0.5 mg of brimonidine and 2.5 mg of timolol maleate were added to the G3.0-PEG-acrylate PBS solution and then the solution was vortexed. Following addition of 25 µL of eosin Y photoinitiator solution (0.1% w/w eosin Y, 40% w/w

triethanolamine, and 4% w/w 1-vinyl-2 pyrrolidinone), the solution was exposed to long-wavelength (365 nm) UV light for 30 min and kept overnight under ambient light prior to use. No further treatment was conducted. The prepared combination drug formulations (brimonidine/timolol/DH) contained 0.1% (w/v) brimonidine and 0.5% (w/v) timolol maleate on the basis of initial loading quantities. Single drug DH formulations (i.e., brimonidine/DH and timolol/DH) were prepared by adding 0.5 mg of brimonidine or 2.5 mg of timolol maleate to 500 µL of 8.1% w/v G3.0-PEG-acrylate PBS solution, mixing the solution with 25 µL of eosin Y photoinitiator solution, and exposing the solution to UV light for 30 min. PBS control formulations (i.e., brimonidine/PBS, timolol/PBS, and brimonidine/timolol/PBS) were prepared by dispersing 0.5 mg of brimonidine and 2.5 mg of timolol maleate individually or in combination in 500 µL of PBS.

3.3.3 Mucoadhesion tests

To assess mucoadhesive properties of DH formulations, zeta potential was measured for quantitative analysis of interaction between mucin particles and DH. To prepare mucin particles, an appropriate amount of gastric porcine mucin was suspended in pH 7.4 PBS and agitated overnight to generate a 1% (w/v) mucin solution. The solution was then subjected to microprobe sonication two times at full power using a Branson Sonifier 450 20kHz model sonication unit(57). 700 µL of mucin particle solution was added to 100 µL of 8.1% (w/v) DH solution. Zeta potential of mucin particles before and after mixing with DH solution was determined using a Malvern ZetaSizer Nano ZS90 (Malvern Instruments Inc, Westborough, MA).

3.3.4 Cytotoxicity assays

To test cytotoxicity of DH formulations, human corneal epithelial cells (HCET, passage # 40) were plated in a 96-well plate at a seeding density of 5000 cells per well and allowed to grow for 24 hours in serum-containing medium. The medium was removed and the cells were incubated in serum free medium (200µL); the DH formulations (30µL each, n=3) were added to the cells or the cells remained untreated (control) for 24 hours. At the end of 24 hours, the media containing the DH formulations was removed and 200 µL of fresh serum free medium was added to each well. 20 µL of 5 mg/ml MTT reagent, dissolved in PBS (pH 7.4), was added to each well and incubated at 37 °C for 4 hours. The medium was aspirated and the resultant formazan crystals were dissolved in 200 µL of dimethyl sulfoxide. The absorbance of the developed color was measured at 540 nm using a microplate reader. An identical set of cells were used for a protein content assay. Protein content was quantified using the Micro BCA Protein Assay Kit (Pierce Biotechnology, Rockford, IL), where bovine serum albumin was used as a standard.

3.3.5 Brimonidine solubility studies

To estimate the degree of solubilization of hydrophobic brimonidine (Sigma-Aldrich, St. Louis, MO) in the DH formulation, an excess amount of brimonidine was added to G3.0-PEG-acrylate PBS solution (8.1% w/v) and vortexed. G3.0-PEG-acrylate was the precursor of the DH and was not treated with UV light to avoid the interfering absorption after formation of a turbid gel. Following overnight equilibration at room temperature, the solution saturated with brimonidine was vortexed again and then centrifuged to remove solid drug residue(56). The supernatant was collected and diluted by a factor of 100 in PBS. Its absorbance value (Y) at 248 nm was recorded on a GENESYS™ 6 UV-Visual spectrophotometer. Thus, drug concentration

[C] (μg/mL) was determined using the following regression equation: [C]=(Y-0.005)/0.063 (58). Following the same procedure, the solubility of brimonidine in plain PBS at room temperature was determined for comparison. Measurements were done in duplicate.

3.3.6 In vitro drug release studies

Drug release studies were performed based on a brimonidine/timolol maleate codrug DH formulation. Briefly, 100 μL of drug-loaded gel solution or eye drop solution was transferred to Spectra/Por® 7 (MWCO 2000) dialysis tubing (Spectrum Laboratories, Inc., CA) and suspended in 1.5 mL of PBS (pH=7.4) containing 0.05% sodium azide in 2 mL microcentrifuge tubes. The tubes were maintained at 37 ± 2 °C and constantly shaken in a shaker incubator. At pre-determined time intervals up to 72 hours, the medium outside the dialysis tube was replaced with 1.5 mL of fresh PBS, which was pre-equilibrated to 37 ± 2°C. The amount of drug released into the dissolution medium was analyzed with LC-MS/MS.

3.3.7 In vitro drug uptake studies

Human corneal epithelial (HCET) cells (passage#40) were seeded in a 48 well-plate at a seeding density of 5000 cells per well and allowed to grow for 24 hours in serum-containing medium. The next day, the cell culture medium was removed and the cells were incubated in serum-free medium (1mL) and the cells were exposed to 150 μL of brimonidine or timolol maleate gel formulation (n=4), whereas the cells exposed to brimonidine and timolol maleate eye drop solutions were used as control. After 1 hour exposure at 37 ºC, the cells were washed twice with 200 μL of cold neutral pH 7.4 PBS and twice with 200 μL of cold acidic pH 5.0 PBS. Cells were lysed by adding 200 μL of 1% (w/v) Triton X-100 solution to each well and allowed to

stand for 30 minutes. The cell lysate was scraped from the plate and a suspension was prepared. To analyze drug concentration, 100 µL of the cell lysate was diluted to 500 µL using acetonitrile, vortexed for 10 minutes, and centrifuged to collect supernatants and cell lysates. The contents of brimonidine and timolol maleate in cell washes, supernatants, and cell lysates were analyzed with LC-MS/MS.

3.3.8 Ex vivo transcorneal transport studies

Corneas were isolated from freshly excised bovine eyes obtained from a local slaughter house, and mounted in Ussing chambers. 50 µL of DH formulation/eye drop formulation (n=5) containing 0.1 % brimonidine (50 µg) and 0.5 % timolol (250 µg) was diluted with assay buffer (pH 7.4) to 1.5 mL and added to the donor side. The following compounds were used for the preparation of assay buffer: NaCl (122 mM), $NaHCO_3$ (25mM), $MgSO_4$ (1.2 mM), K_2HPO_4 (0.4 mM), $CaCl_2$ (1.4 mM), HEPES (10 mM), and glucose (10 mM). At 1, 2, 3, 4, and 6 h, 200 µL of sample solution was collected on the receiver side and then immediately replaced with 200 µL of fresh assay buffer. At 6 hours, sample solutions on both sides were collected, and the tissues were removed from the chambers. Drug contents in the sample solutions were analyzed with LC-MS/MS.

3.3.9 Ex vivo drug uptake studies

Freshly excised bovine eyes were rinsed with PBS and incubated in a muffin pan partially filled with PBS, as per a previously reported method(59). A solution of gel formulation or eye drop formulation (50 µL) (n=4) was administered to the corneal surface and allowed to drain. Every 15 minutes, 50 µL of fresh PBS was instilled as an eye drop to simulate tear exposure and

to maintain corneal moisture. At 1 hour, the bovine eyes were dissected to collect aqueous humor and corneal tissues including epithelium, stroma, and endothelium. Drug contents in the excised eye tissues were quantified using LC-MS/MS.

3.3.10 Drug extraction and recovery

A liquid-liquid method for extraction of brimonidine and timolol from bovine ocular tissues was first validated to determine the percentage extraction recovery of brimonidine and timolol (Table 3.1). An extraction recovery study was performed at 500 ng/mL of analytes for all the corneal layers isolated in this study. Briefly, 20 mg of each tissue (epithelium, stroma, endothelium; n = 5) was weighed in a glass tube. 20 µL of standard analyte solution containing 25 µg/mL of timolol and brimonidine, 10 µL of dorzolamide solution (25 µg/mL) as internal standard (IS) and 470 µL of 2 % NaOH solution (pH 12.8) was added to the above tube. Since both analytes as well as IS are highly basic molecules, 2 % NaOH solution was used to keep them under unionized state. Tissues were homogenized using a hand homogenizer on an ice bath followed by sonication for 10 minutes. To the tissue homogenates 4 ml of ethyl acetate/dichloromethane mixture (1:1 v/v) was added. The mixture was vortexed for 15 minutes and then subjected to centrifugation for 10 minutes to collect the organic layer. The organic layer was blow-dried with nitrogen at 40 ºC. The residue, after evaporation, was reconstituted with 1 mL of acetonitrile-water (75:25 v/v) and subjected to LC-MS/MS analysis. The percentage extraction recovery was calculated using the following formula:(analyte concentration detected in the tissue ×100)/(initial concentration of the analyte used).

Table 3.1 The percent extraction recovery (%) of brimonidine and timolol maleate at 500 ng/mL from bovine corneal epithelium, stroma, and endothelium (n=5)

Tissue	Brimonidine	Timolol maleate
Corneal epithelium	123.0 ± 21.7	103.0 ± 17.6
Corneal stroma	118.0 ± 41.2	120.0 ± 10.1
Corneal endothelium	112.0 ± 17.7	114.0 ± 26.0

3.3.11 Drug quantification in ex vivo uptake studies

After validating the percentage extraction recovery of the liquid-liquid extraction method, drug content in the tissue samples from *ex vivo* uptake study was estimated. Ocular tissues were weighed and mixed with 490 µL of 2 % NaOH and 10 µL of 25 µg/mL dorzolamide (internal standard) in 10 mL glass tubes, followed by the same procedure as mentioned in the extraction and recovery section. To analyze drug levels in the aqueous humor, 50 µL of aqueous humor (~ 48 mg) was diluted 5 times with acetonitrile-water mixture (75:25 v/v) containing dorzolamide as an internal standard and subjected to LC-MS/MS analysis. A final concentration of the internal standard was maintained at 250 ng/mL for all processed samples as well as standard samples used for preparing the calibration curve.

3.3.12 LC-MS/MS analysis

LC-MS/MS was applied to determine the concentrations of brimonidine and timolol maleate. An API-3000 triple quadrupole mass spectrometry (Applied Biosystems, Foster City, CA, USA) coupled with a PerkinElmer series-200 liquid chromatography (Perkin Elmer, Walthm, Massachusetts, USA) system was used. Analytes were separated on Zorbax extended C18 column (2.1 x 50 mm, 5 µm) using 5 mM ammonium formate in water (A) and acetonitrile (B) as mobile phase. The linear gradient elution at a flow rate of 0.3 ml/min with total run time

of 6 min was as follows: 60% A (0–1.0min), 10% A (2.0– 4.0 min), and 60% A (4.5-6.0 min). Brimonidine, timolol and dorzolamide (internal standard) were analyzed in positive ionization mode with the following multiple-reaction monitoring (MRM) transitions: 292 → 212 (brimonidine); 317 → 261 (timolol); and 325 → 199 (dorzolamide).

3.3.13 Statistical analysis

Data were analyzed with analysis of variance (ANOVA) followed by t-test for pairwise comparison of subgroups using SigmaPlot 11.0 (Systat Software Inc., San Jose, CA). *P* values <0.05 were considered statistically significant.

3.4 Results

3.4.1 Characterization of dendrimer hydrogel (DH) formulations

Intermediate OH-PEG-acrylate and final product G3.0-PEG-acrylate (Scheme 1) were characterized with FT-IR. As shown in Figure 1, a broad absorption band at 3199-3678 cm^{-1} was attributed to O-H stretching of the hydroxyl end group of PEG. A strong absorption band at 2889 cm^{-1} was attributed to C-H stretching of PEG. The presence of acrylate group of PEG was confirmed by an absorption band at 1728 cm^{-1} corresponding to C=C stretching and a band at 1650 cm^{-1} corresponding to C=O stretching. Because of the remaining primary amine groups on the dendrimer surface, a broad absorption band at 3125-3166 cm^{-1} indicates N-H stretching. PEG was coupled to PAMAM dendrimer via an amide linkage. The C=O stretching band at 1650 cm^{-1} became stronger due to the formation of amide linkages and indicates the success of the coupling reaction.

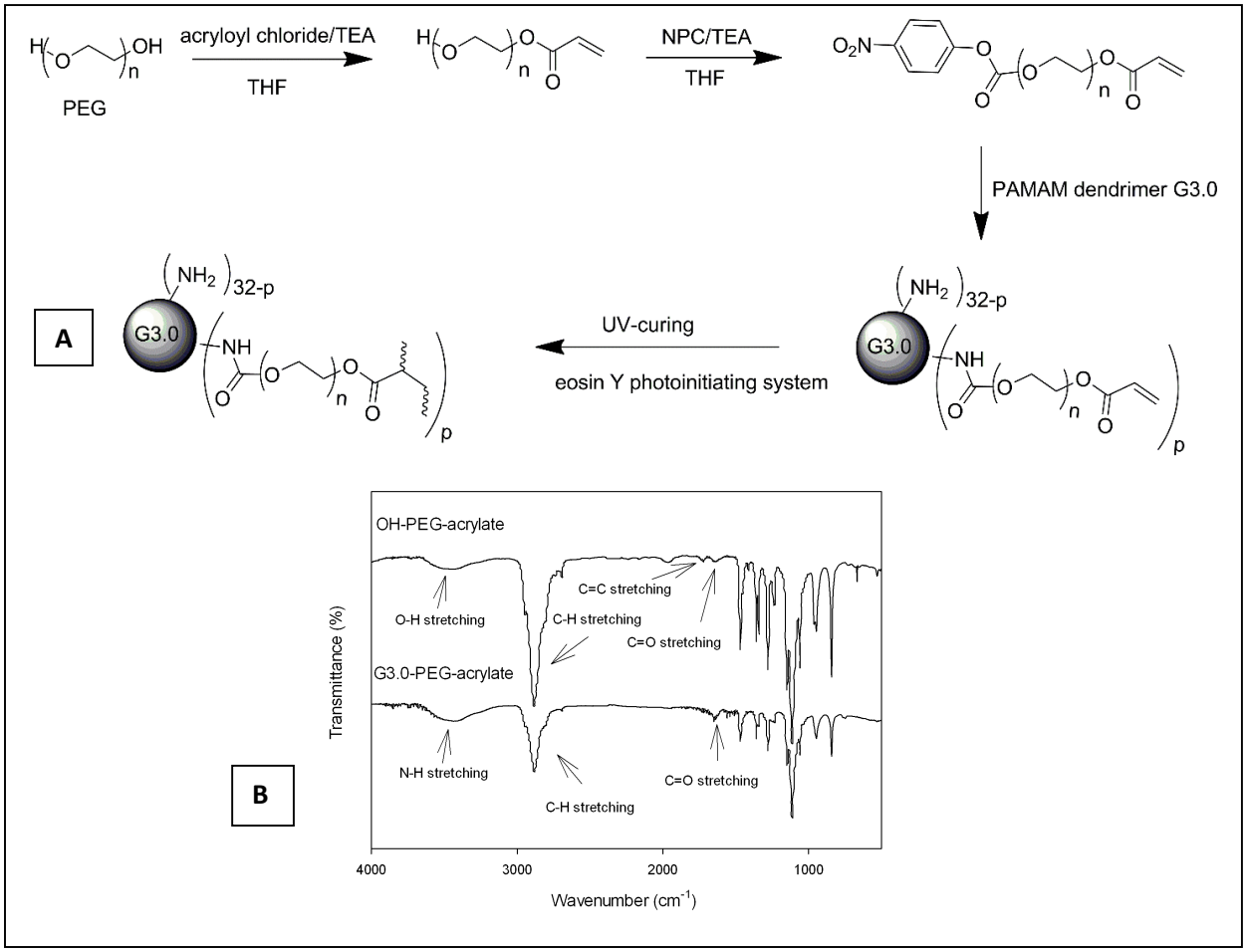

Figure 3.2 Synthesis route (A) and FT-IR spectrum (B) of G3.0-PEG acrylate conjugates.

As a viscous gel solution is preferred to solid gel in ocular drug delivery due to its ease of handling and application, PAMAM dendrimer G3.0 coupled with an average of 3 PEG-acrylate chains was used to make viscous gel solutions for preparation of anti-glaucoma drug formulations. Mucoadhesiveness of DH formulation was demonstrated by zeta potential measurements. The zeta potential of 1% w/v mucin particles in PBS was -7.13±0.77 mv. The zeta potential changed to -3.6±1.50mv after mixing with DH solution. This shift towards zero

was attributed to the aggregation of mucin particles as a result of adsorption of DH on the mucin particles(57).

The effect of plain DH formulations on cellular response was assessed. According to the MTT assay (Figure 3.3), the DH formulation including photoinitiator neither caused toxicity to HCET cells nor induced cell proliferation rate. The protein content in the cells was quantified by using the Micro BCA protein assay kit. It was shown that the protein content in the cells treated with the DH formulation was just 9.3% less than in the control.

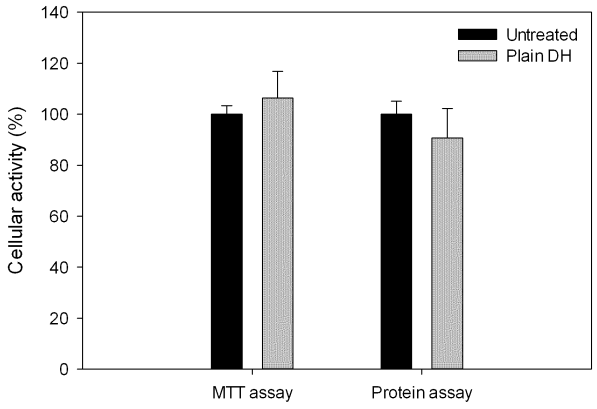

Figure 3.3 Effects of DH gel formulation on HCET cellular activity in comparison with the control. MTT assay and BCA Protein Assay Kit(Pierce)

3.4.2 Drug water solubility enhancement

It has been documented that PAMAM dendrimers are able to increase the water solubility of hydrophobic compounds by encapsulating them inside the hydrophobic core(20). PEGylation can augment the water solubility enhancement properties of dendrimers presumably due to stabilizing and shielding effects of the PEG layer(17, 56). As dendrimers have been integrated into a hydrogel network, one envisioned property of a dendrimer hydrogel is its ability to encapsulate hydrophobic drug molecules inside the dendritic cores, while simultaneously allowing the loading of hydrophilic drugs in the PEG network. To test the ability of the

dendrimer hydrogel to enhance water solubility of hydrophobic drugs, brimonidine was used in this work. Unlike the commonly used water-soluble brimonidine tartrate in ophthalmic solutions, brimonidine has a limited solubility in aqueous solutions. Our studies revealed that the solubility of brimonidine was 392 μg/mL in plain PBS. In sharp contrast, the solubility of brimonidine dramatically increased to 696 μg/mL in DH formulation, representing a 77.6% increase.

3.4.3 In vitro drug release studies

DH formulation resulted in extended *in vitro* release of brimonidine and timolol maleate. It was observed that drug release was sustained for nearly 72 hours for brimonidine (Figure 3.4-A) and nearly 56 hours for timolol maleate (Figure 3.4-B). Contrastingly, drug in eye drop formulations was released quickly. Both brimonidine and timolol maleate were released completely from eye drop formulations within 90 minutes, indicating the eye drop formulations did not sustain the drug release. Sustained drug release from DH formulations was attributed to the entrapment of drug molecules in the PEG network and the encapsulation by the nanodomains inside the dendrimers.

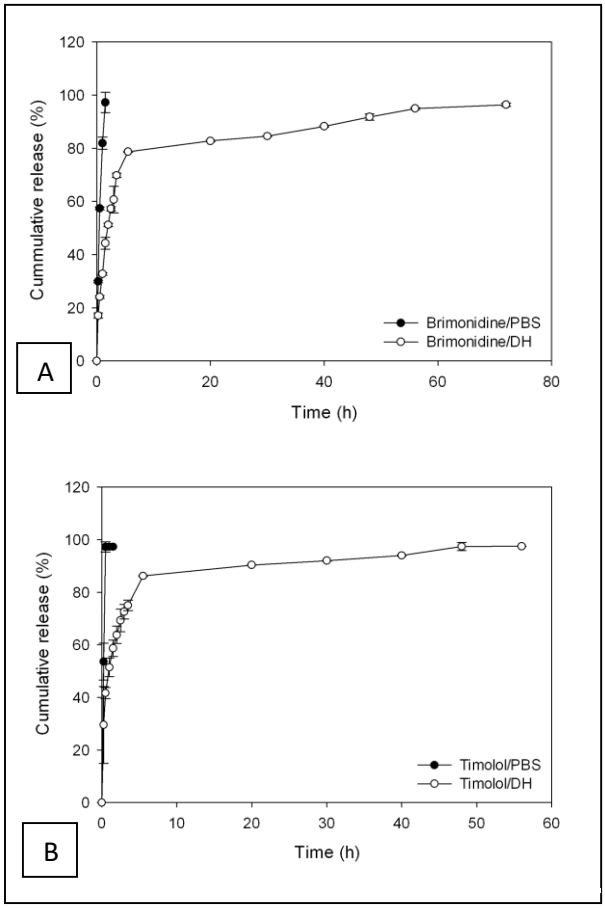

Figure 3.4 In vitro release of brimonidine (A) and timolol maleate (B) in pH 7.4 PBS at 37C

3.4.4 Enhanced drug uptake

The intracellular uptake of brimonidine and timolol maleate by HCETs was substantially increased by the DH formulations. According to the analysis of drug content in the cells treated with the DH and eye drop formulations(Figure 3.5), the eye drop brought about an uptake of 3.81±0.28 % for brimonidine and 49.40±2.60 % for timolol maleate, respectively. With the aid of DH formulations, brimonidine uptake was 76.17±19.47 % and timolol uptake was 69.10±13.70 %. The uptake of hydrophobic brimonidine mediated with the DH formulation was 19-fold higher than its uptake mediated with the eye drop formulation ($P = 0.003$). This dramatically enhanced cellular uptake of brimonidine was attributed to its increased water solubility and its even dispersion in the gel network.

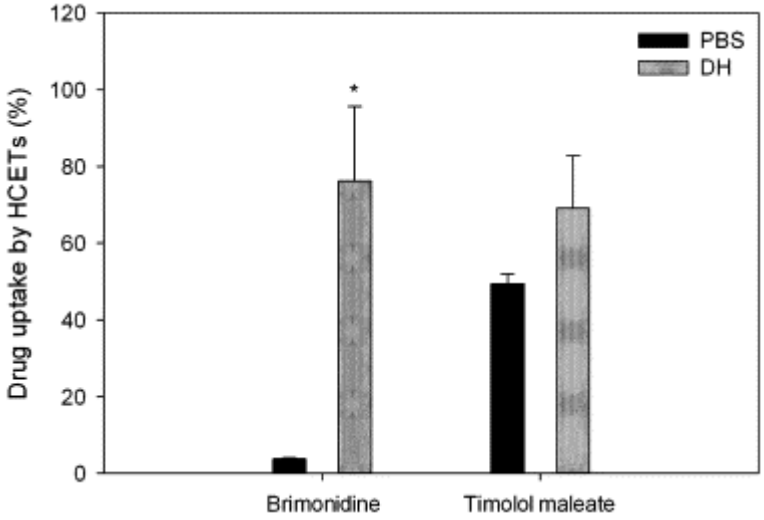

Figure 3.5 Drug uptake in HCET cells treated with DH and eye drop formulations.

3.4.5 Ex vivo transcorneal transport

Transcorneal transport of anti-glaucoma drugs was also enhanced by the DH. Brimonidine and timolol maleate crossed the cornea at a significantly higher rate with the application of the DH formulation. For brimonidine, statistically significant differences ($p < 0.05$) were observed in its transcorneal transport starting from 3 hours (Figure 3.6-A). For

timolol maleate, statistically significant differences ($p < 0.001$) were observed in its transcorneal transport starting from 2 hours (Figure 3.6-B). At 6 hours, 1.06±0.18 % of brimonidine had cumulatively transported across the cornea, while 13.54±1.83 % of timolol maleate had

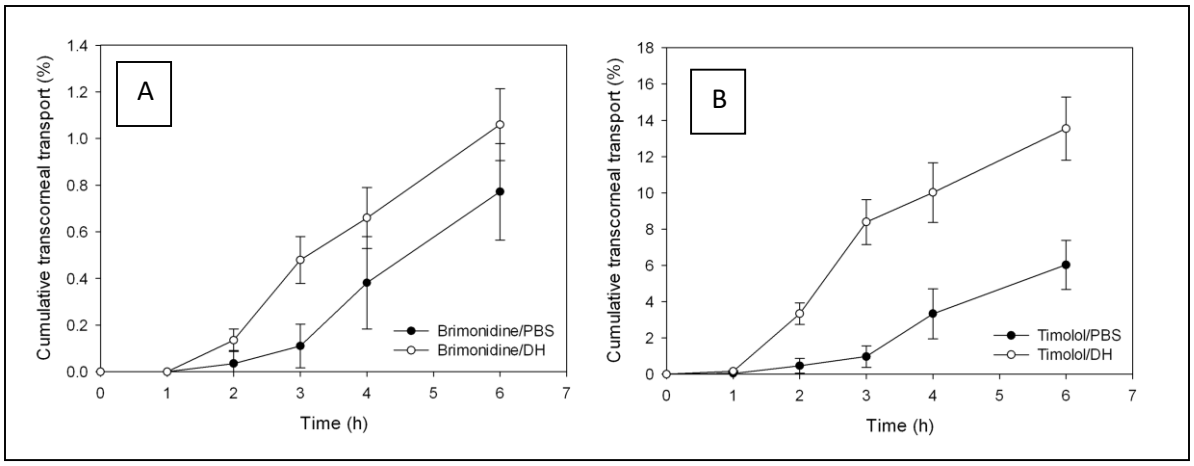

Figure 3.6 Cumulative transport of brimonidine (A) and timolol maleate (B) mediated with DH and eye drop formulations across the bovine cornea.

cumulatively transported across the cornea. In contrast, the eye drop formulation only resulted in cumulative transport of 0.77±0.23 % for brimonidine and 6.03±1.55 % for timolol maleate. The cumulative transport of timolol maleate was much higher than that of brimonidine at the end of 6 hours, regardless of formulation type. This might be attributed to the differences in drug physicochemical properties such as LogD, which is the most critical parameter influencing transcorneal drug transport.

3.4.6 *Ex vivo* eye uptake

This study was conducted to assess the *ex vivo* uptake of brimonidine and timolol maleate in ocular tissues after 1 hour of topical instillation. The levels of brimonidine from the hydrogel formulation were similar to those from the eye drop solution formulation in corneal epithelium, stroma, and endothelium (Figure 3.7-A). We observed significantly higher levels of timolol maleate from the hydrogel formulation as compared to the eye drop solution in corneal

epithelium, stroma, and endothelium (Figure 3.7-B). Particularly, the timolol maleate levels from the hydrogel formulation were 4.6-fold higher in epithelium, 2.6-fold higher in stroma, and 0.4-fold higher in endothelium. However, significant difference in drug level was not observed in the aqueous humor between hydrogel formulation and eye drop formulation for both brimonidine and timolol maleate (Figure 3.7-A and Figure 3.7-B), which may be due to the short contact time of the formulation with the eye surface and the short duration of the study (1 hour).

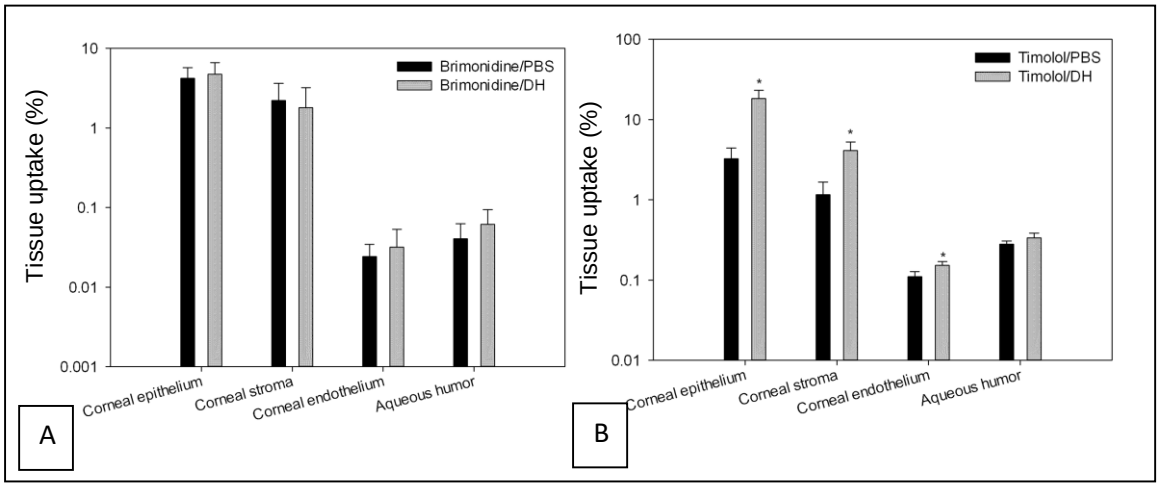

Figure 3.7 Uptake of brimonidine (A) and timolol maleate (B) in bovine corneal epithelium, stroma, endothelium, and aqueous humor after 1hr topical instillation of DH and eye drop formulations (N=4).

3.5 Discussion

Recently, we have synthesized photocurable dendrimer derivatives, which are PAMAM dendrimers tethered with multiple polyethylene glycol (PEG) chains and photoreactive acrylate groups. Exposing dendrimer-derivatives to UV light triggers crosslinking of the reactive acrylate groups, leading to the formation of a DH network. DH integrates the characteristics and properties of both a dendrimer and PEG network. The surface charges conferred by terminal groups on the dendrimer surface can make the hydrogel polyionic with controllable charge density. The interior, hydrophobic core of the dendrimer can encapsulate hydrophobic

compounds, dramatically increasing their water solubility and loading amounts. Concurrently, the crosslinked PEG network can load hydrophilic drugs.

In our previous approach, PEG chains were conjugated to amine-terminated PAMAM dendrimer first and then photoreactive acrylates were introduced to the dendrimer by reacting acryloyl chloride ideally with the hydroxyl end groups of PEG chains(15). Acrylate attached to PEG would respond to UV light exposure to initiate crosslinking reaction. This approach has proven to be valid for gel formation. Due to the possible shielding effect of PEG, acrylate groups on the dendrimer surface should be avoided in order to achieve efficient crosslinking. However, restricting acrylate groups to the distal end of the conjugated PEG chains was beyond control in that approach as acryloyl chloride has reactivity towards free amine group on the dendrimer surface. In this work, we modified this approach by reacting acryloyl chloride with PEG diol first, to ensure that acrylate was restrictively attached to the end of PEG, and then by coupling PEG acrylate to the dendrimer. Photoreactive dendrimer derivatives in aqueous solutions are able to become viscous solutions and/or form "no flow" gels *in situ* upon light exposure by tuning their concentration and/or structure parameters including the degree of PEGylation, PEG length, and the density of acrylate groups on the dendrimer.

DH was investigated as a new platform for anti-glaucoma drug delivery. The DH formulations displayed good cytocompatibility and could dramatically enhance water solubility of hydrophobic anti-glaucoma drugs such as brimonidine. Brimonidine and timolol maleate encapsulated into DH were released in a sustained manner. The intracellular uptake of brimonidine and timolol maleate by HCETs and their transport across the bovine corneal endothelium were substantially increased by DH formulations as opposed to eye drop solution formulations. According to *ex vivo* bovine eye studies, significantly higher levels of timolol

maleate in corneal epithelium, stroma and endothelium resulted from the application of the gel formulation. PAMAM dendrimer is known to transiently open tight junctions in the intestinal epithelium(60). Thus, one possible explanation for the higher uptake in the DH formulations is the temporary disruption of the tight junctions in the corneal epithelial cell layer. The *in vitro* and *ex vivo* studies indicate that dendrimer hydrogel formulations are capable of enhancing delivery of anti-glaucoma drugs and represent a novel platform to deliver drugs for the treatment of ocular diseases such as glaucoma. As a consequence, reduced dosing frequency and sustained efficacy of ocular drugs are expected and will be studied in future work.

Chapter 4 Surface Engineering of Macrophages with Nanoparticles to Generate a Cell-Nanoparticle Hybrid Vehicle for Drug Delivery

The following chapter is adapted from a manuscript accepted in the International Journal of Nanomedicine: Published 22 December 2009, Volume 2010(5), Pages 25-36, DOI: https://doi.org/10.2147/IJN.S8339

4.1 Abstract

Tumors frequently contain hypoxic regions that result from a shortage of oxygen due to poorly organized tumor vasculature. Cancer cells in these areas are resistant to radiation- and chemo-therapy, limiting the treatment efficacy. Macrophages have inherent hypoxia-targeting ability and hold great advantages for targeted delivery of anticancer therapeutics to cancer cells in hypoxic areas. However, most anticancer drugs cannot be directly loaded into macrophages because of their toxicity. In this work, we designed a novel drug delivery vehicle by hybridizing macrophages with nanoparticles through cell surface modification. Nanoparticles immobilized on the cell surface provide numerous new sites for anticancer drug loading, hence potentially minimizing the toxic effect of anticancer drugs on the viability and hypoxia-targeting ability of the macrophage vehicles. In particular, quantum dots and 5-(aminoacetamido) fluorescein-labeled polyamidoamine dendrimer G4.5, both of which were coated with amine-derivatized polyethylene glycol, were immobilized to the sodium periodate-treated surface of RAW264.7 macrophages through a transient Schiff base linkage. Further, a reducing agent sodium cyanoborohydride was applied to reduce Schiff bases to stable secondary amine linkages. The distribution of nanoparticles on the cell surface was confirmed by fluorescence imaging, and it was found to be dependent on the stability of the linkages connecting nanoparticles to the cell surface.

4.2 Introduction

The cell membrane, a semipermeable lipid bilayer, defines the cell boundary and consists of lipids, proteins and carbohydrates that are responsible for selective uptake of molecules, cell-cell interactions, cell-matrix interactions, and many other vital cell activities. Because of the importance of cell surface interactions to cell and tissue function, various cell surface engineering

approaches have been explored to modify the cell surface to manipulate cell behavior and function(61, 62).

Considerable progress has been made in introducing non-native chemical species to the cell membrane permitting a wide range of applications in biology, medicine, drug delivery, and tissue engineering(36). A molecule of interest can be attached to the cell surface through a fatty tether including GPI-anchored proteins(63) and cholesterol-tethered compounds(64). A viable alternative is to apply enzyme-catalyzed chemical reactions to modify carbohydrates on the cell surface. For example, existing surface glycoforms can be utilized as acceptors for reactions with an exogenously applied glycosyltransferase and appropriate activated sugar donor(61, 65). Sialic acids are the most common terminal sugar residue on the cell surfaces and play an important role in cell adhesion and recognition. Unnatural sialic acid precursors can be incorporated into cell surface glycoforms by metabolic engineering(66). Direct covalent reactions can also be applied to enable chemical modification of cell surfaces(67, 68). One possible approach is to couple biomolecules of interest to the cell surface via reactive cell surface groups such as aldehydes and ketones(35, 69). The generation of these reactive cell surface groups may be achieved by direct chemical or enzymatic treatment, or by the metabolic incorporation of an unnatural molecule that contains the chosen chemical species.

Cell surface engineering has generated tremendous advantages for drug delivery and tissue engineering. For example, a synthetic adenovirus receptor inserted to the cell surface via a metabolic engineering approach facilitates the entrance of adenovirus into cells that are normally resistant to infection by this virus(70). Uptake of exogenous proteins could be enhanced by inserting appropriate synthetic receptors(71). Selectively killing tumor cells could be realized by controlling the targeting of an antibody through tagging tumor cells with a non-natural sugar into

the polysialic acid molecules on the cell surface(72). Cell surface modification approaches have also been applied to generate three-dimensional cell aggregates or tissue-engineered constructs through cell crosslinking(73). A recent study reported that polyethylene glycol (PEG) can be attached to the surface of islets to circumvent immune rejection during transplantation of pancreatic islets from donor to a patient(68).

In this work, we designed a novel hypoxia-targeted drug delivery vehicle by hybridizing macrophages with nanoparticles through cell surface modification. Tumors frequently contain hypoxic regions that result from a shortage of oxygen due to poorly organized tumor vasculature. Cancer cells in these areas are resistant to radiation- and chemo-therapy, limiting the treatment efficacy(29). Macrophages and monocytes have inherent hypoxia-targeting ability and hold great advantages for selective delivery of anticancer therapeutics to cancer cells in hypoxic areas(27, 29, 74, 75). However, most anticancer drugs cannot be directly loaded into macrophages or monocytes because of their toxicity. Hybridizing a macrophage cellular vehicle with a synthetic carrier, particularly nanoparticles, may represent a novel approach for effective delivery of anticancer drugs to hypoxic regions in solid tumors. Immobilizing nanoparticles on the cell surface provide numerous new sites for anticancer drug loading, hence potentially minimizing the toxic effect of anticancer drugs on the viability and hypoxia-targeting ability of the macrophage or monocyte vehicles.

The focus of the current work was to demonstrate the feasibility of immobilizing nanoparticles including polyamidoamine (PAMAM) dendrimers and quantum dots (Qdots) to the macrophage surface through cell surface chemical modification. Dendrimers are highly branched macromolecules with low polydispersity and well-defined surface functionality. Utility of dendrimers in this work allowed us to take advantage of their versatility to explore optimal

approaches for cell-nanoparticle hybridization and realize a high drug payload and assembly of multiple functional entities necessary for hybridization and drug delivery. Commercially available quantum dots coated with amine-derivatized PEG was also studied for cell-nanoparticle hybridization. Qdots have been explored for fluorescence imaging of living cells(76). Although the limited number of surface groups of Qdots is not advantageous for drug loading, hybridizing cells with Qdots possessing long-term photostability offers a noninvasive way for cell tracking *in vivo* and would provide further evidence to demonstrate the feasibility of the cell nanoparticle hybridization approach explored in this work.

4.3 Experimental

4.3.1 Materials

Qdot® 525 ITK™ amino (PEG) quantum dots(QD525) and 5-(aminoacetamido) fluorescein (AAF) were purchased from Invitrogen (Carlsbad, CA). PAMAM G4.5 dendrimer was purchased from Dendritech (Midland, MI). PEG diamine (MW= ~ 3350 g mol^{-1}), N-hydroxysuccinimide (NHS), 1-ethyl-3-(3-dimethylaminopropyl) carbodiimide hydrochloride (EDC), sodium phosphate buffer (10×), sodium periodate ($NaIO_4$), and sodium cyanoborohydride ($NaCNBH_3$) were purchased from Sigma-Aldrich (St. Louis, MO). 4',6-diamidino-2-phenylindole (DAPI), Dulbecco's modified Eagle medium (DMEM), sodium hydroxide, paraformaldehyde, phosphate-buffered saline (PBS), fetal bovine serum (FBS), penicillin, and Trypan blue were purchased from Fisher Scientific (Pittsburgh, PA).

4.3.2 Preparation of AAF-labeled PEGylated G4.5 dendrimers (AAF-G4.5-PEG)

Synthesis

The synthesis of G4.5-PEG followed our previous work[21].[19] Upon removal of methanol from G4.5 PAMAM stock solution by rotary evaporation, G4.5 PAMAM dendrimer (5 mg) was dissolved in 2 mL of sodium PBS (0.1 M, pH=5.5). To this solution were added 5.4 mg of EDC and 3.2 mg of NHS. After a 15 minute reaction at room temperature, 68.5 mg of PEG diamine (MW= ~ 3350 g mol^{-1}) predissolved in the buffer solution was added to the reaction solution dropwise. Then 1.4 mg of AAF predissolved in the buffer was slowly added to the reaction solution. The reaction mixture solution was stirred in the dark overnight. The resultant AAF-G4.5-PEG nanoparticles were purified by dialysis and then freeze dried.

Proton nuclear magnetic resonance (^{1}H NMR) spectroscopy

The ^{1}H NMR spectra of dendrimer derivatives were recorded on a Varian Mercury-300 MHz NMR spectrometer (Varian, Palo Alto, CA). The solvent used was deuterium water (D_2O), which has a chemical shift of 4.8 ppm.

Fluorescence spectroscopy

Fluorescence emission spectra of AAF and AAF-G4.5-PEG in water were recorded on a Varian Cary Eclipse fluorescence spectrophotometer with an excitation wavelength of 488 nm.

4.3.3 Preparation of macrophage-nanoparticle hybrid vehicles

As illustrated in Figure 4.1, nanoparticles (Qdots or AAF-G4.5-PEG) were coupled to the surface of macrophages via either a transient Schiff base linkage or a stable secondary amine linkage.

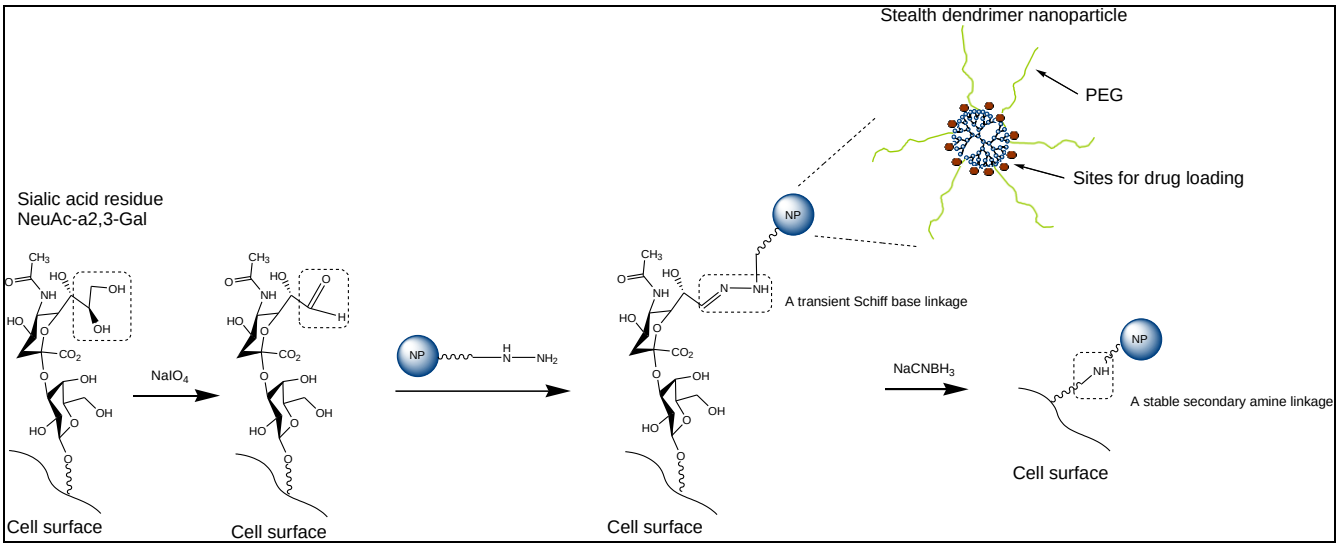

Figure 4.1 Hybridization of nanoparticles and macrophage through cell surface modification. Sialic acid residues on the cell surface are modified with sodium periodate to generate aldehydes. Aldehydes react with amine group of PEG conjugated to the nanoparticle surface to form Schiff bases. Schiff bases can be further reduced to stable secondary amine linkages using sodium cyanoborhydride.

Macrophage-nanoparticle hybrids with a transient linkage (macrophage-T-nanoparticle hybrids)

RAW264.7 macrophages were plated on coverslips at a density of 1.2×10^4 cells/well. At 70% confluence, the cells were treated with 0.1 mM cold $NaIO_4$ in 100 µL PBS(pH 7.4), incubated with shaking for 15 minutes at 4 °C in the dark, and then rinsed with cold PBS three times to remove $NaIO_4$.(73). Following the $NaIO_4$ treatment, the cells were incubated with 12 µg of nanoparticles dissolved in 100 µL of PBS for 0-24 hours. The resultant macrophage-T-nanoparticle hybrids were washed with PBS and incubated in PBS. At predetermined time points, macrophage-T-nanoparticle hybrids were fixed with 300 µL 4% paraformaldehyde for

fluorescence or confocal imaging. Untreated macrophages incubated with nanoparticles were used as a control.

Macrophage-nanoparticle hybrids with a stable linkage (macrophage-S-nanoparticle hybrids)

Macrophage-T-nanoparticle hybrids were further treated with 100 µL 0.1 mM $NaCNBH_3$ for 1~2 hours to convert the transient Schiff base linkages to stable amide linkages, washed with PBS, and incubated in PBS. At predetermined time points, macrophage-T-nanoparticle hybrids were fixed with 4% paraformaldehyde for imaging. Untreated macrophages incubated with nanoparticles were used as a control.

4.3.4 pH-dependent cell viability assay

Since RAW264.7 macrophages were subjected to surface modification and the rate of the stabilizing amide reaction is pH-depdendent, the effect of pH of modifying solutions on their viability was studied. In brief, RAW264.7 macrophages were initially incubated for two hours in media of different pH values including DMEM (pH 7.4, control) and PBS (pH 8, pH 9 and pH 10, adjusted with sodium hydroxide), washed with PBS (pH 7.4) three times, and grown in DMEM supplemented with 10% FBS and 5% penicillin for 48 hours. Viable cells were counted by using the Trypan blue assay. In addition, toxicity of 0.1mM $NaCNBH_3$ in DMEM at pH 7.4 was also evaluated. Cell viability (%)= total number of viable cells in each group/total number of viable cells in the control × 100.

4.3.5 Fluorescence image analysis

True-color fluorescence images of the macrophage-nanoparticle hybrids were taken under a Zeiss Axiovert 200 inverted fluorescence microscope (Carl Zeiss AG, Oberkochen, Germany) or with a Leica TCS-SP2 AOBS confocal laser scanning microscope(Leica, Solms, Germany). DAPI nuclear stain was applied for colocalization of nanoparticles. Images were analyzed with ImageJ software (National Institutes of Health, Bethesda, MD).

4.4 Results and Discussion

4.4.1 Preparation of macrophage-nanoparticle hybrids

In this study commercial QD525 quantum dots coated with an amine-derivatized PEG layer and synthesized PEGylated carboxyl-terminated PAMAM dendrimer G4.5 were employed for hybridization with macrophages. PEGylated G4.5 PAMAM dendrimer was labeled with AAF to allow confirmation of immobilization of nanoparticles on the cell surface by fluorescence imaging. Polyanionic G4.5 PAMAM dendrimer has a relatively high number of surface groups, negligible toxicity and immunogenicity, and favorable biodistribution(77). The negatively charged dendrimers have demonstrated negligible cellular uptake due to their low non-specific interaction with the negatively charged cell surface. Inclusion of PEG provides dendrimers with favorable pharmacokinetic and tissue distribution and reduces potential accumulated toxicity and immunogenicity of the nanoparticles. Importantly, PEG helps nanoparticles to escape from phagocytosis of macrophages. This is a critical step for constructing the proposed hybrid delivery system. PEGylated dendrimers of larger molecular weight and with more branches tend to have a lower accumulation in cells as demonstrated previously(78).

Similarly to the QD525 employed in this study, PEGylated G4.5 was designed to have amine-derivatized PEG chains on the surface, based on which cell surface modification chemistry was explored. PEGylated dendrimers have been well characterized previously(38, 39, 56, 79, 80). According to the ^{1}H-NMR measurement, an average of eight PEG chains were coupled to G4.5. PEGylated G4.5 was labeled with a moderately water-soluble fluorescence probe, AAF. As shown in Figure 4.2, AAF coupled to the dendrimer has an emission wavelength of 515 nm, which is identical to the emission wavelength of AAF. The unaltered emission wavelength of AAF following this coupling strategy was also found in a previous report(81). Furthermore, the fluorescence emission intensity of AAF coupled to PEGylated G4.5 is significantly higher than that of AAF prepared in water at saturation, suggesting that AAF coupled to PEGylated G4.5 has higher water solubility than its unmodified form. The increase in the water solubility of AAF was attributed to the successful conjugation of AAF to the PEGylated dendrimer.

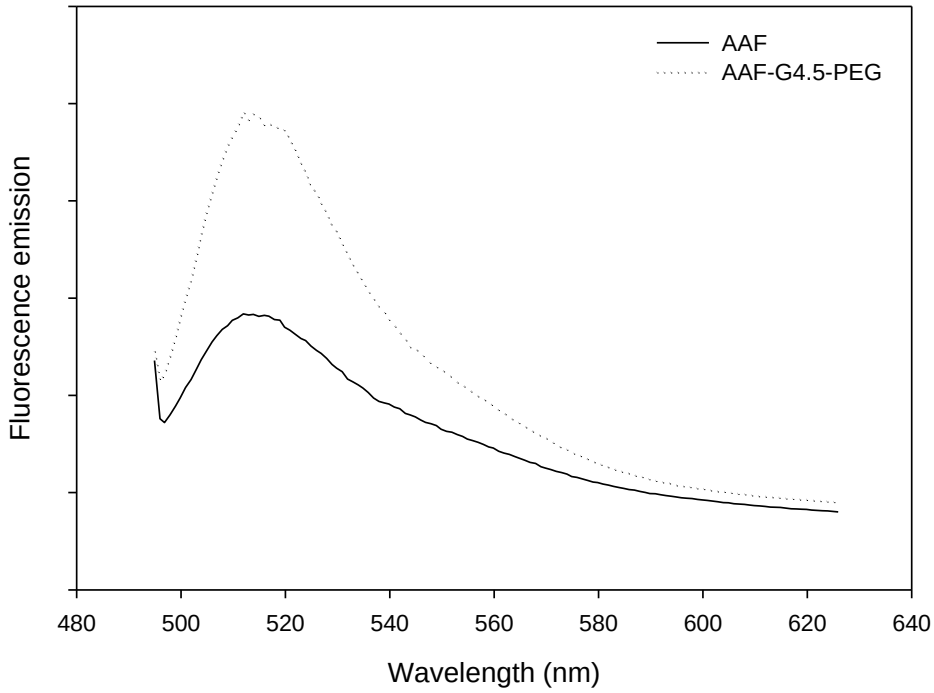

Figure 4.2 Fluorescence emission spectra of AAF and AAF-G4.5-PEG.

A number of methods have been developed to enable the chemical modification of cell surfaces. In this project, we employed a simple and well-documented methodology to immobilize nanoparticles to the macrophage cell surface. In particular, sialic acid residues embedded on the cell surface were converted to aldehydes with sodium periodate. Our results showed that the toxicity of $NaIO_4$ was negligible at the concentration of 0.1 mM. This was supported by the work of Ong and coworkers(73). Aldehydes reacted with primary amine end groups of PEG on the nanoparticle surface to form Schiff bases. Schiff base linkage is labile and can be cleaved in aqueous solution by hydrolysis. Accordingly, the macrophage-T-nanoparticle hybrids constructed are expected to readily release nanoparticles through the cleavage of the transient Schiff base linkages. We also applied a reducing agent, sodium cyanoborohydride, to reduce Schiff bases to stable secondary amine linkages(37). It has been reported that sodium cyanoborohydride has high specificity toward the Schiff base. According to our cell viability studies (Figure 4.3), sodium cyanoborohydride at 0.1 mM was nontoxic to RAW264.7 macrophages. As the reaction proceeds more efficiently at basic pH(82). the viability of RAW264.7 macrophages at high pH (8-10) was evaluated to determine whether the immobilization chemistry can be performed at high pH. As shown in Figure 4.3, pH affects the cell viability. The viability of RAW264.7 macrophages remains intact at pH 8 or pH 7.4 with sodium cyanoborohydride. The cell viability dropped slightly to 88% at pH 9. By contrast, the viability was reduced drastically to 52% at pH 10. The results suggest that mild basic pH has a minimal impact on the viability of RAW264.7 macrophages and the optimum pH within that range can be explored for increasing the immobilization efficiency.

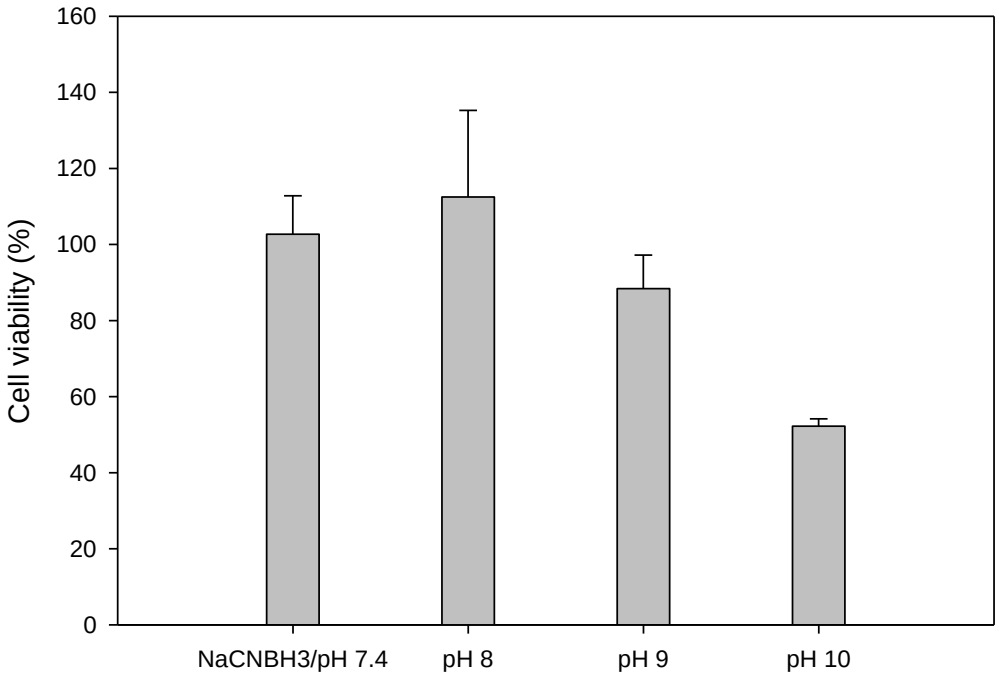

Figure 4.3 pH-dependent viability of RAW264.7 macrophages. Cells were incubated for two hours at the indicated pH and then assessed by the Trypan blue assay 48 hours later. Nontoxicity of 0.1mM sodium cyanoborohydride in DMEM at pH 7.4 was confirmed. Note: Bar = SD. Abbreviations: DMEM, Dulbecco's modified Eagle's medium.

4.4.2 Fluorescence image analysis of macrophage-Qdot hybrids

Fluorescence microcopy and confocal microscopy were applied to confirm the hybridization of nanoparticles with macrophages. As shown in Figure 4.4, both macrophage-T-nanoparticle hybrids and macrophage-S-nanoparticle hybrids prepared with QD525 exhibit strong fluorescence intensity at the edge of the cells, clearly outlining the cell surface. Qualitatively, more QD525 were taken up in macrophage-T-nanoparticle hybrids as opposed to macrophage-S-nanoparticle hybrids, reflecting the stability of the linkage between the nanoparticles and the cell. Confocal microscopy images in z-sections were taken to further examine the distribution of QD525 over the course of time. Without cell surface modification, QD525 were phagocytosed quickly and evenly distributed in the cytoplasm (Figure 4.5-A 4h and 14h). Although QD525 were still internalized, a significant amount of QD525 accumulated at the edge of the cells treated with

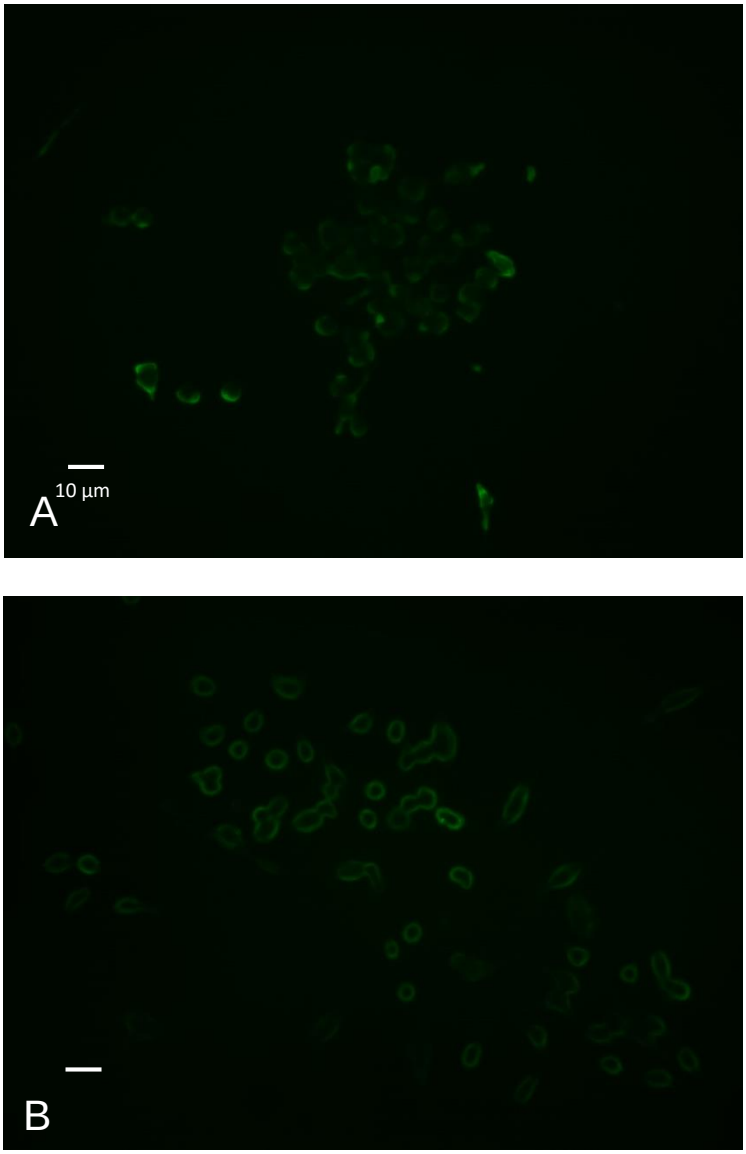

Figure 4.4 Fluorescence microscopy images of macrophage-Qdot hybrids. A) Macrophage-T-Qdot. B) Macrophage-S-Qdot. Original magnification 400x, scale bar 10 µm.

sodium periodate (Figure 4.5-B) or a combination of sodium periodate and sodium cyanoborohydride (Figure 4.5-C). QD525 immobilized on the cell surface through a stable secondary amine bond displayed good stability overnight (Figure 4.5-C-14h). In contrast, QD525 linked to the cell surface via Schiff base linkages were found to be re-distributed in the cell overnight (Figure 4.5-B-14h).

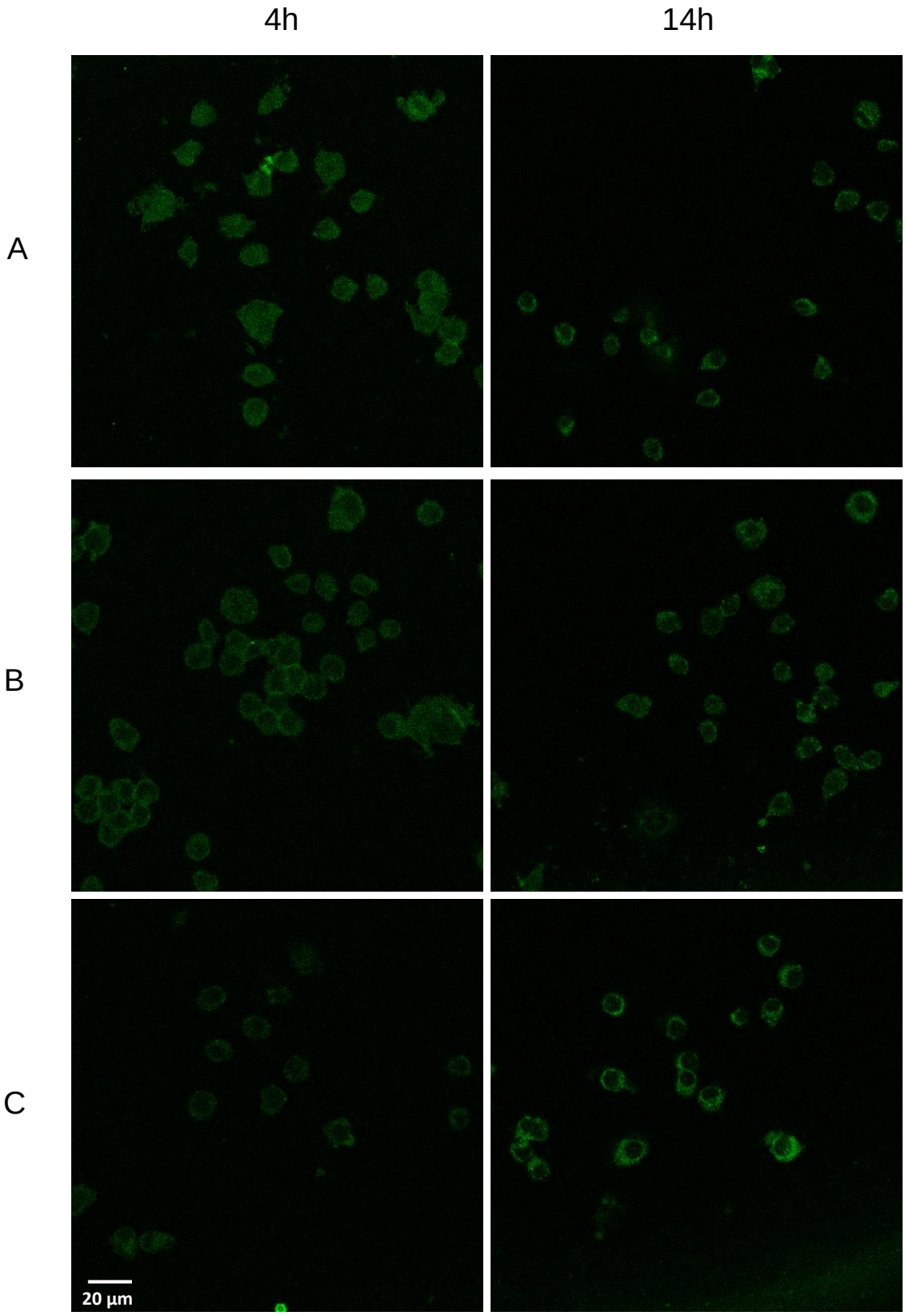

Figure 4.5 Confocal microscopy images (630×) of macrophage-Qdot hybrids at 4 hours (left panel) or 14 hours (right panel) post treatment. A) Qdots incubated with untreated macrophages (control); B) Macrophage-T-Qdot hybrids;(C) Macrophage-S-Qdot hybrids.

4.4.3 Fluorescence image analysis of macrophage-dendrimer hybrids

Macrophages hybridized with AAF-labeled PEGylated PAMAM dendrimer G4.5 were also studied. As shown in Figure 4.6-A, the level of the internalization of AAF-G4.5-PEG by untreated macrophages is low. This confirmed that cationic surface charges and PEGylation indeed helped to reduce nonspecific internalization by macrophages. Further, an apparently biased distribution of AAF-G4.5-PEG nanoparticles was observed on the cell surface of macrophages that were treated with sodium periodate (Figure 4.6-B) or the combination of sodium periodate and sodium cyanoborohydride (Figure 4.6-C). A significant increase in fluorescence intensity of macrophage-T-dendrimer hybrids and macrophage-S-dendrimer hybrids as compared to the control suggests that more dendrimer nanoparticles have been immobilized to the cell surface and/or internalized by the cells. The amine linkages connecting dendrimers to the cell enabled macrophage-S-dendrimer hybrids to carry dendrimers stably on the surface for an extended period of time. We also observed that when the surface-treated RAW264.7 macrophages were incubated with the same amount of AAF-G4.5-PEG (12 µg), a condition of a high concentration (12 µg/100 µL) and a short incubation (1 minute) and that of a low concentration (12 µg /1.5 mL) and a long incubation (10 minutes) resulted in a similar hybridization efficiency as determined by confocal microscopy measurements. Cell viability remained good during the surface treatment.

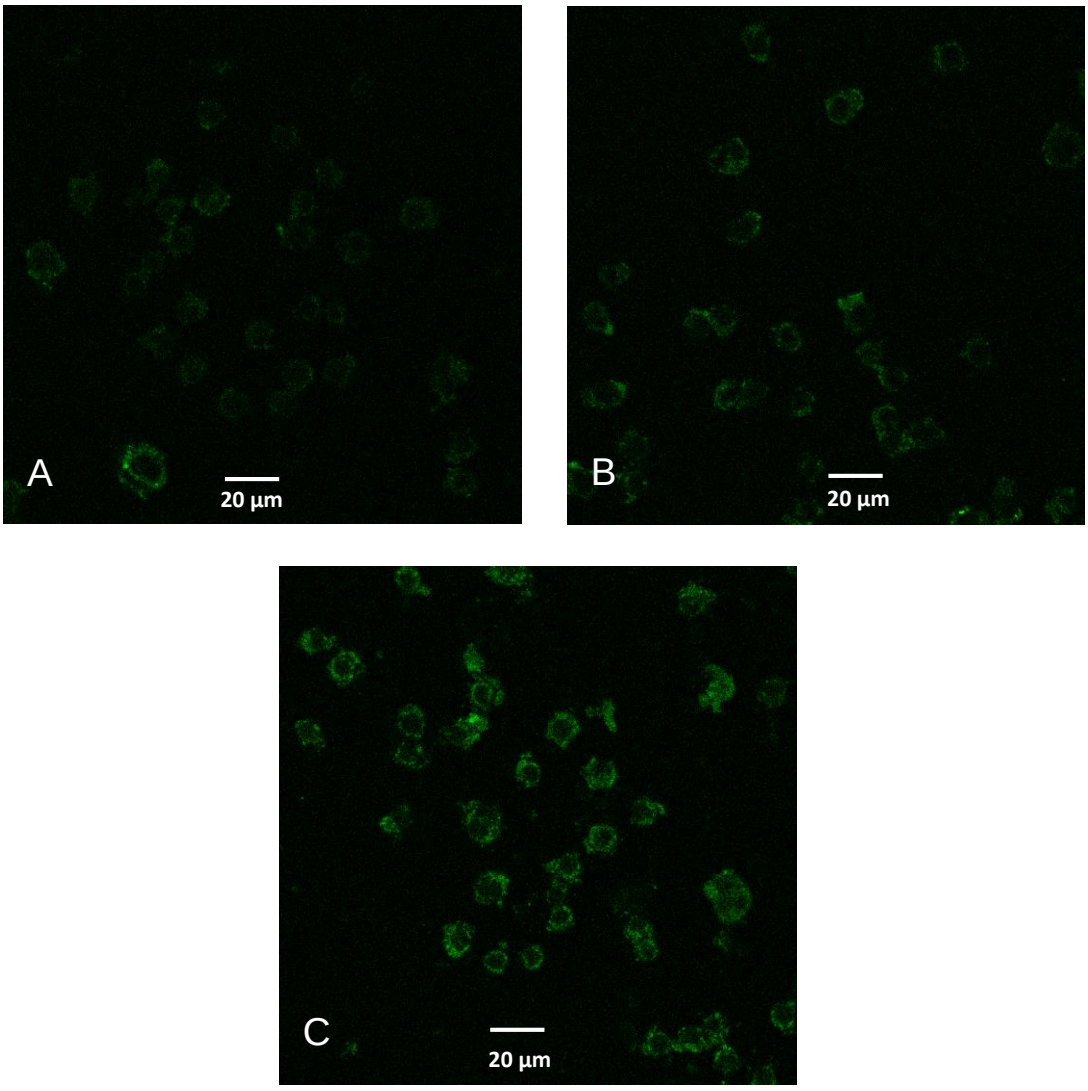

Figure 4.6 Confocal microscopy images (630×) of macrophage-dendrimer hybrids. (A) Untreated macrophages incubated with AAF-G4.5-PEG for 10 minutes and fixed immediately(control); (B) Macrophage-T-dendrimer hybrids fixed immediately following 10 minute incubation with AAF-G4.5-PEG; (C) Macrophage-S-dendrimer hybrids fixed at 14 hours following treatment of sodium cyanoborohydride.

To further evaluate the intracellular localization of nanoparticles, we performed a colocalization assay on AAF-G4.5-PEG with nuclear DAPI staining. Clearly shown in Figure 4.7-A, a significant amount of AAF-G4.5-PEG nanoparticles were internalized within one-minute incubation and accumulated evenly in the cytoplasma with no selectivity towards the cell surface after overnight culture. Entry of the nanoparticles into nuclei was also observed in the macrophages. This became more evident when the cells were incubated with AAF-G4.5-PEG for

an extended period of time (overnight incubation, Figure 4.7-B). In addition, more nanoparticles were internalized by the cells following the overnight incubation as indicated by the increase in the fluorescence intensity. Macrophage-S-dendrimer hybrids (Figure 4.7-D) show a stronger fluorescence intensity at the cell surface and less in nuclei as compared to macrophage-T-dendrimer hybrids (Figure 4.7-C), confirming that the stability of immobilized dendrimers in macrophage-S-dendrimer hybrids was higher than macrophage-T-dendrimer hybrids.

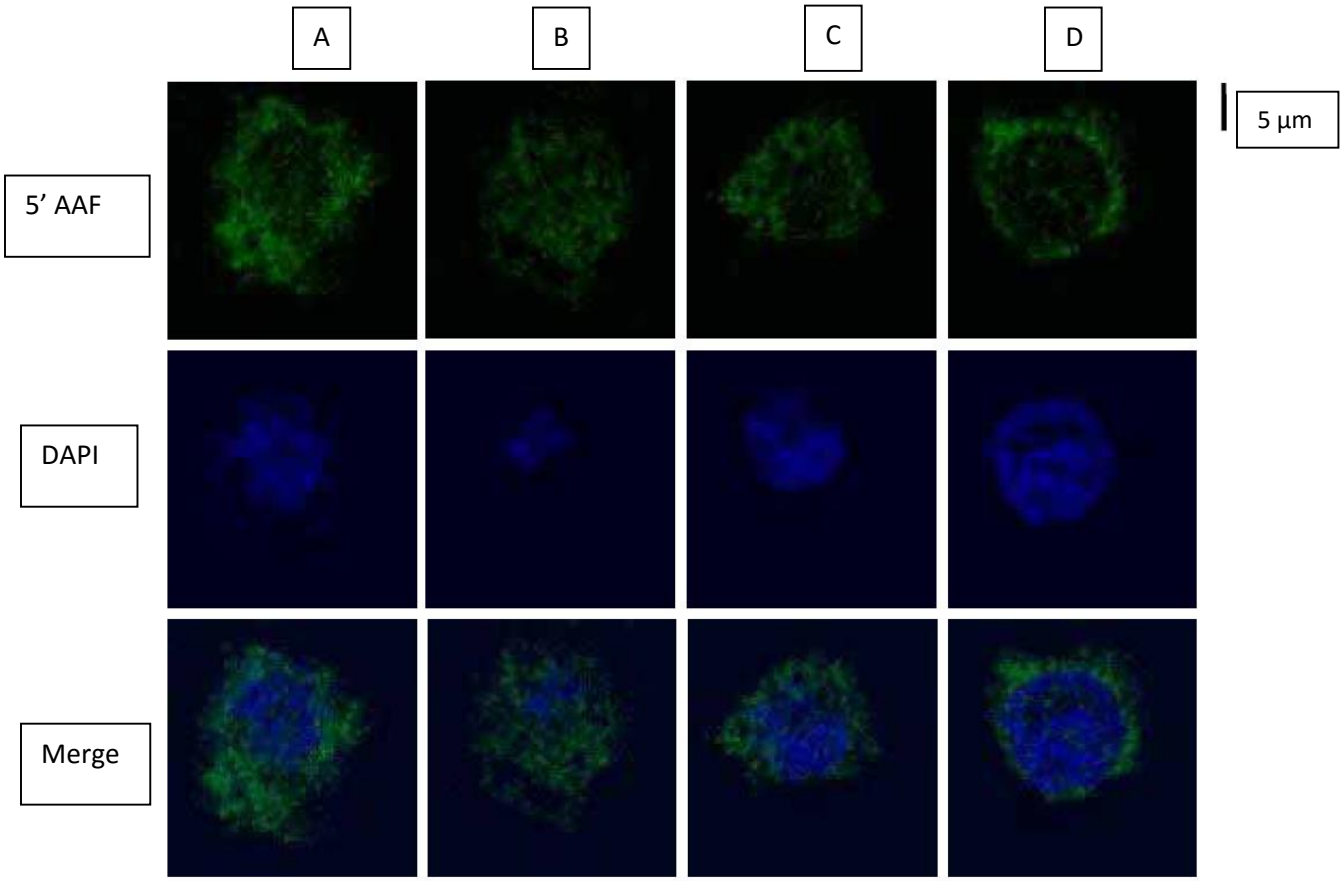

Figure 4.7 Colocalization assay of AAF-G4.5-PEG (green) with nuclei (blue) by confocal microscopy (630×). (A) Control 1: untreated macrophages incubated with AAF-G4.5-PEG for 1 minute, cultured overnight (24 hours), then fixed and counterstained with DAPI; (B) Control 2: untreated macrophages incubated with AAF-G4.5-PEG overnight (24 hours), then fixed and counterstained with DAPI; (C) Macrophage-T-dendrimer hybrids: sodium periodate-treated macrophages incubated with AAF-G4.5-PEG for 1 minute, cultured overnight (24 hours), then fixed and counterstained with DAPI; (D) Macrophage-S-dendrimer hybrids: sodium periodate-treated macrophages incubated with AAF-G4.5-PEG for 1 minute, treated with sodium cyanoborohydride, cultured overnight (24 hours), then fixed and counterstained with DAPI.

It is apparent that fluorescently labeled nanoparticles were taken into the macrophages after each treatment. Qualitatively, there is a uniform distribution of fluorescence throughout the

untreated control groups, suggesting cellular uptake pathways are responsible for this occurrence. Following surface modification, a pronounced ring of fluorescence is observed towards the cell surface. Quantitative analysis of the distribution of nanoparticle fluorescence was attempted with the intensity profiled generated by ImageJ software (Figure 4.8). Since all confocal images were taken under identical image acquisition settings, the fluorescence intensity profiles-generated allowed us to quantitatively analyze fluorescence distribution in individual cells based on their relative fluorescence intensity. For each group, three representative cells were chosen and analyzed. Individual cells were measured three times from different orientations with each orientation approximately bisecting midlines. From each profile, intensity values were recorded from fluorescence peaks at the two cell boundaries and from a fluorescence peak near the midline of each trace. The results are summarized in Table 4.1. The results from the intensity traces show that for a nanoparticle incubation of 1 minute there is a 20.8% more fluorescence at the cell boundaries versus the cell center. For an overnight nanoparticle incubation, there was an even distribution of fluorescent intensity where the cell walls exhibited a fluorescence value that was 99.8% of the fluorescence of the midpoint of the slice. Surface modification drastically increased the ratio of fluorescence between the cell walls versus the cell interior. The macrophage-T-nanoparticle hybrids showed an 85.2% increase in fluorescence near the cell exterior, whereas the macrophage-S-nanoparticle hybrids showed a 94.4% increase in cell wall fluorescence. Based on these measurements we show that there is markedly more fluorescence near the cell surface for surface-treated groups, whereas there is an even distribution of nanoparticles in the control groups.

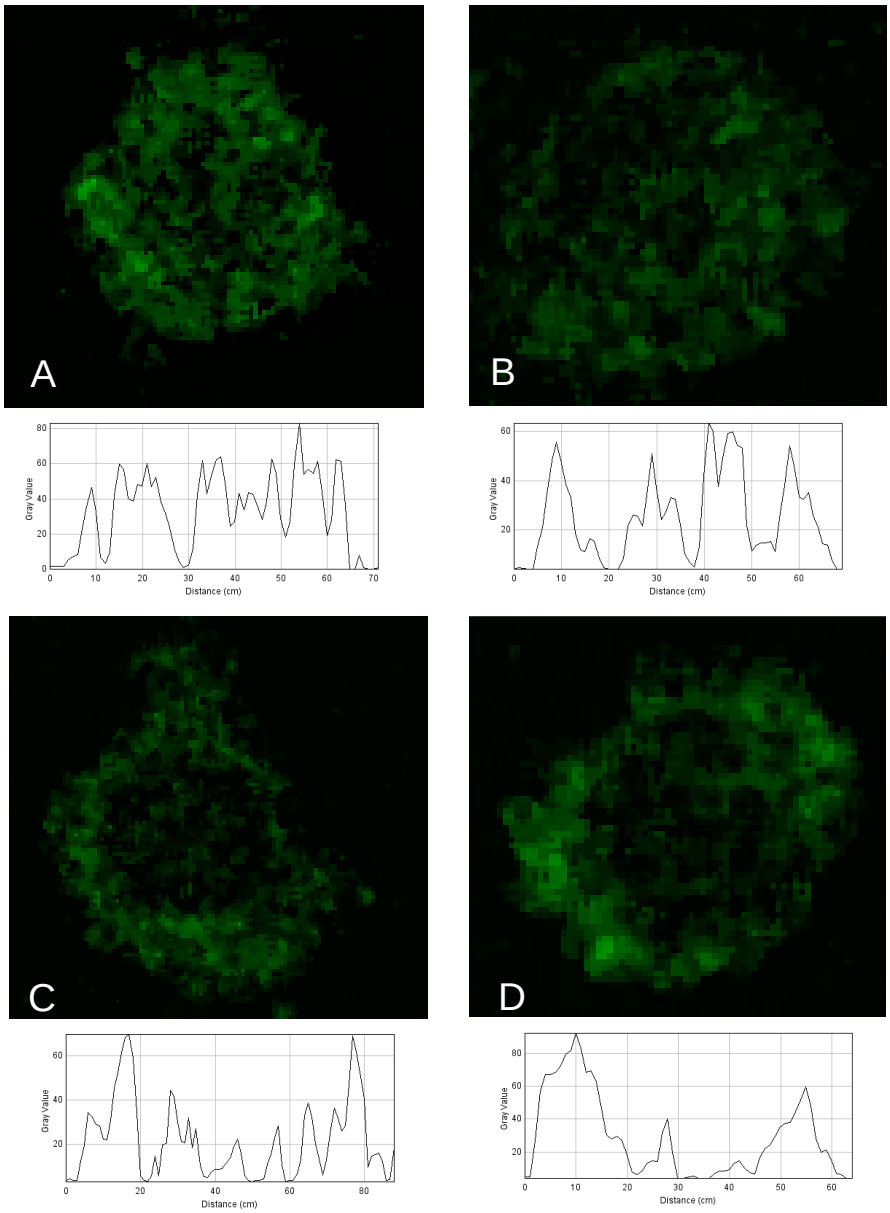

Figure 4.8 Quantitative analysis of the distribution of fluorescence intensity in representative cells. (A) Control 1; (B) Control 2; (C) Macrophage-T-dendrimer hybrid; (D) Macrophage-S-dendrimer hybrid. The treatment conditions are detailed in Figure 4.7

Table 4.1 Summary of the distribution of AAF fluorescence intensity in macrophages subjected to various treatments as indicated below.

Group	[L]	[I]	[R]	([L]+[R])/[I] (%)
A	70.3±12.5	55.0±3.7	62.6±7.3	120.8
B	58.4±10.6	57.8±13.5	57.0±6.4	99.8
C	64.3±10.2	33.4±8.7	59.3±12.5	185.2
D	67.5±8.1	33.6±5.2	63.2±6.1	194.4

(A) Control 1; (B) Control 2; (C) Macrophage-T-dendrimer hybrid; (D) Macrophage-S-dendrimer hybrid (The treatment conditions are detailed in Figure 4.7). [L], average fluorescence intensity at the left cell wall; [I] average fluorescence intensity at the interior of the cell; [R], average fluorescence intensity at the right cell wall. The original images (n=3) were analyzed with ImageJ.

4.5 Future work

From a chemistry perspective, this work demonstrated the proof-of-principle of chemically hybridizing nanoparticles with macrophages through cell surface modification. The reaction conditions explored in this study were mild to the cells. It should be noted that internalization of nanoparticles by macrophages seems to be an inevitable process because of their innate phagocytic capability. Nonetheless, our studies disclosed that cell surface modification provides a means to retard the internalization progress and alter the intracellular distribution of nanoparticles. A comprehensive understanding of the trafficking and dynamic distribution of nanoparticles is needed in order for us to optimize the hybridization process. Reducing nonspecific phagocytic internalization of nanoparticles will be pursued in our laboratory. The sizes of the QD525 and PAMAM dendrimers as an important factor affecting nanoparticle internalization by cells will be studies. PAMAM dendrimers have a versatile structure ideal for construction of drug delivery systems and have been extensively studied by many groups, including us(17, 18, 83, 84). Future work will include hybridization of drug-carrying dendrimers and/or QD525 with macrophages and studying the delivery efficiency of such a new drug vehicle in terms of drug distribution in hypoxic areas using *in vitro* spheroid models and animal models.

4.6 Conclusions

QD525 and dendrimers were immobilized to the macrophage cell surface either through a transient Schiff base linkage or a stable amine linkage. The distribution of nanoparticles on the cell surface was confirmed by fluorescence imaging and was found to be dependent on the stability of the linkages connecting nanoparticles to the cell surface. Achieving homogeneous distribution of anticancer drugs within tumors remains one of the major challenges in cancer chemotherapy and is critical for treatment effectiveness. The current study has explored an innovative way of utilizing nanoparticles and cellular vehicles for anticancer drug delivery. Development of a cell-nanoparticle hybrid vehicle through cell surface modification would utilize the best aspects of both cellular carriers and nanoparticles and may help to improve anticancer drug distribution and penetration in tumors.

4.7 Acknowledgements

This research was supported in part by The Jeffress Memorial Trust (J-873) and the National Institutes of Health (R21NS063200). RAW264.7 macrophages were provided by Dr. Xianjun Fang (Department of Biochemistry & Molecular Biology, Virginia Commonwealth University). Confocal microscopy was performed at the VCU Department of Neurobiology & Anatomy Microscopy Facility, supported, in part, with funding from NIH-NINDS Center core grant (5P30NS047463).

Chapter 5 Summary and Continuing Work

This work explored the use of PAMAM dendrimers in two drug-delivery systems. These preliminary studies have provided promising results for continuing the work on dendrimers in hydrogels and in cell-surface engineering.

5.1 DH formulations

DH formulations were shown to increase the loading of drug molecules, increase transcorneal drug delivery, and exhibit sustained-delivery of drug molecules. These DHs show potential to reduce dosing frequency through sustained-delivery and increase drug bioavailability through increased precorneal residence and transcorneal transport. The *in vitro* and *ex vivo* studies explored in this work set the stage for continued experiments *in vivo*.

Based on the work in this thesis, IOP-lowering ability and sustained-delivery of concomitant DH was studied in rabbits. Continued work combined poly(lactic-*co*-glycolic acid) (PLGA) nanoparticles in DH formulations; this work found sustained drug levels of brimonidine and timolol maleate for one week following a single dose in rabbit ocular tissues. This PLGA-DH system also led to a sustained IOP reduction of 18% or higher for 4 days. This platform shows continuing promise for treating chronic eye diseases, including glaucoma(85).

This project has evolved from the use of a photoinitiator and UV-curing system based on concerns of potential hazards and stability issues of the DH formulations. The Eosin-Y photoinitiator and UV system works on the mechanism of creating free radicals for crosslinking

within the PEG network and free radicals can be harmful to tissues, so a newer system has been devised and tested to avert these issues. New work focuses on the creation of electrospun dendrimer-PEG nanofiber mats (DNF) with the incorporation of poly(ethylene oxide) in a single drug formulation of brimonidine tartrate. Compatibility and efficacy of the DNFs were studied in rats over a three week period. It was found that DNFs and eye drop formulations had similar responses after single doses; however, DNF formulations showed increased efficacy attributed to accumulation of dendrimers in the anterior chamber of the eye over the three week trial(86, 87).

In related work on dendrimer hydrogels in our lab, a new approach to hydrogel synthesis utilizes biorthogonal chemistry. This work uses copper-free click chemistry for the crosslinking of DH as an alternative approach to potentially disruptive photoinitiators. Click chemistry uses the high reactivity of alkynes towards azides for efficient coupling of synthetic molecules. Using this click chemistry approach, dendrimers were loosely entangled in a physical network for the sustained delivery of drug molecules. This approach offers catalyst-free chemistry and is highly customizable for use in a variety of applications(87).

5.2 Cell-surface modified macrophages

In this work, distribution of nanoparticles on RAW264.6 cell surfaces was observed by fluorescence microscopy and was found to be dependent on the stability of the linkages tethering nanoparticles to the cell surface. The current work explored the proof-of-concept for a novel approach to loading anti-cancer drugs onto immune cells via PAMAM dendrimers. Future work includes optimization of the hybridization conditions, synthesis of anti-cancer drug-loaded dendrimers, quantification of macrophage-dendrimer drug-loading capacity, and studying the infiltration of hybridized-macrophages into tumor models. The results from this study, indicate

that a hybridized cellular delivery system is feasible and could potentially improve drug-targeting in a range of applications.

References

1. American Academy of Ophthalmology [Internet]. Eye Health Statistics [cited 2017 June]. Available from: https://www.aao.org/newsroom/eye-health-statistics

2. World Health Organization [Internet]. Visual impairment and blindness: Fact Sheet No 282 2014 Aug[cited 2017 June]. Available from: http://www.who.int/mediacentre/factsheets/fs282/en

3. Kingman S. Glaucoma is second leading cause of blindness globally. Bull World Health Organ. 2004 Nov;82(11):887-88.

4. Kapetanakis V, Chan MPY, Foster PJ, Cook DG, Owen CG, Rudnicka AR. Global variations and time trends in the prevalence of primary open angle glaucoma (POAG): a systematic review and meta-analysis. Br J Ophthalmol. 2016 Jan;100(1):86-93.

5. Tham YC, Li X, Wong TY, Quigley HA, Aung T, Cheng CY. Global prevalence of glaucoma and projections of glaucoma burden through 2040: A systematic review and meta-analysis. Ophthalm. 2014 Nov;121(11):2081-90.

6. Jonas JB, Aung T, Bourne RR, Bron AM, Ritch R, Panda-Jonas S. Glaucoma. The Lancet. 2017 May.

7. Zhang K, Zhang L, Weinreb RN. Ophthalmic drug discovery: novel targets and mechanisms for retinal diseases and glaucoma. Nature Reviews Drug Discovery. 2012 Jul;11(7):541-59.

8. Dave VS, Bhansali SG. Pharmacokinetics and pharmacodynamics of ocular drugs. In: Pathak Y, Sutariya V, Hirani AA, editors. Nano-Biomaterials For Ophthalmic Drug Delivery. Springer International Publishing; 2016. p. 111-29.

9. Kaur IP, Smitha R. Penetration enhancers and ocular bioadhesives: two new avenues for ophthalmic drug delivery. Drug Dev Ind Pharm. 2002 Apr;28(4):353-69.

10. Vandamme TF, Brobeck L. Poly(amidoamine) dendrimers as ophthalmic vehicles for ocular delivery of pilocarpine nitrate and tropicamide. J Control Release. 2005;102(1):23-38.

11. Arnott S, Fulmer A, Scott WE, Dea ICM, Moorhouse R, Rees DA. The agarose double helix and its function in agarose gel structure. J Mol Biol. 1974 Dec;90(2):269-284.

12. Yoshioka H, Mori Y, Tsukikawa S, Kubota S. Thermoreversible gelation on cooling and on heating of an aqueous gelatin poly(N-isopropylacrylamide) conjugate. Polym Adv Technol. 1998 Feb;9(2):155-58.

13. Demirci U, Khademhosseini A, editors. Gels handbook : Fundamentals, properties and applications. Singapore: New Jersey: World Scientific; 2016.

14. Dingels C, Frey H. From Biocompatible to biodegradable: poly(ethylene glycol)s with predetermined breaking points. Adv Polym Sci. 2013 Oct;262:167-190.

15. Desai PN, Yuan Q, Yang H. Synthesis and characterization of photocurable polyamidoamine dendrimer hydrogels as a versatile platform for tissue engineering and drug delivery. Biomacromol. 2010 Mar;11(3):666-73.

16. Klajnert B, Bryszewska M. Dendrimers in medicine. New York: New York : Nova Science; 2007.

17. Sarkar K, Yang H. Encapsulation and extended release of anti-cancer anastrozole by stealth nanoparticles. Drug Deliv. 2008;15(5):343-46.

18. Yang H, Lopina ST. Stealth dendrimers for antiarrhythmic quinidine delivery. J Mater Sci: Mat in Med. 2007;18(10):2061-65.

19. Durairaj C, Kadam RS, Chandler JW, Hutcherson SL, Kompella UB. Nanosized dendritic polyguanidilyated translocators for enhanced solubility, permeability, and delivery of gatifloxacin. Invest Ophthalmol Vis Sci. 2010;51(11):5804-16.

20. Milhem OM, Myles C, McKeown NB, Attwood D, D'Emanuele A. Polyamidoamine starburst dendrimers as solubility enhancers. Int J Pharm. 2000;197:239-41.

21. Matsumura Y, Maeda H. A new concept for macromolecular therapeutics in cancer chemotherapy: mechanism of tumoritropic accumulation of proteins and the antitumor agent smancs. Cancer Res. 1986 Dec;46(12):6387-92.

22. Maeda H, Wu J, Sawa T, Matsumura Y, Hori K. Tumor vascular permeability and the EPR effect in macromolecular therapeutics: a review. J Contr Release. 2000;65(1):271-84.

23. Cutrera J, Shulin L. Passive and active tumor homing cytokine therapy. In: Lustgarten J, Cui Y, Li S, editors. Targeted Cancer Immune Therapy. Springer; 2009. p. 99-102.

24. van Vlerken LE, Vyas TK, Amiji MM. Poly(ethylene glycol)-modified nanocarriers for tumor-targeted and intracellular delivery. Pharm Res. 2007;24(8):1405-14.

25. Andreesen R, Hennemann B, Krause SW. Adoptive immunotherapy of cancer using monocyte-derived macrophages: Rationale, current status, and perspectives. J Leukoc Biol. 1998 Oct;64(4):419-426.

26. Vignola AM, Gjomarkaj M, Arnoux B, Bousquet J. Monocytes. J Allergy Clin Immunol. 1998;101(2):149-52.

27. Griffiths L, Binley K, Iqball S. The macrophage - a novel system to deliver gene therapy to pathological hypoxia. Gene Ther. 2000 Feb;7(3):255-262.

28. Turpin J, Lopez-Berestein G. Differentiation, maturation, and activation of monocytes and macrophages: functional activity is controlled by a continuum of maturation. In: Lopez-Berestein G, Klostergaard, J., editors. Mononuclear Phagocytes in Cell Biology. CRC Press, Inc; 1993. p. 70-77.

29. Brown JM, Wilson W. Exploiting tumour hypoxia in cancer treatment. Nat Rev Cancer. 2004 Jun;4(6):437-47.

30. Jougasaki M, Ichiki T, Takenoshita Y, Setoguchi M. Statins suppress interleukin-6-induced monocyte chemo-attractant protein-1 by inhibiting Janus kinase/signal transducers and activators of transcription pathways in human vascular endothelial cells. Brit J Pharmac. 2010 Mar;159(6):1294-1303.

31. Yamashiro S, Takeya M. Tumor-derived Monocyte Chemoattractant Protein-1 induces intratumoral infiltration of monocyte-derived macrophage subpopulation in transplanted rat tumors. Amer J Path. 1994;145(4):856-67.

32. Zhang Y, Shi J, Li Y. Cardiomyocyte death in doxorubicin-induced cardiotoxicity. Arch Immunol Ther Exp. 2009;57(6):435-45.

33. Zhou S, Starkov A, Froberg MK. Cumulative and irreversible cardiac mitochondrial dysfunction induced by doxorubicin. Cancer Res. 2001 Jan;61(2):771-77.

34. Mellor H, Callaghan R. Accumulation and distribution of doxorubicin in tumour spheroids: the influence of acidity and expression of P-glycoprotein. Cancer Chemo and Pharm. 2011;68(5):1179-90.

35. De Bank PA, Kellam B, Kendall DA, Shakesheff KM. Surface engineering of living myoblasts via selective periodate oxidation. Biotechnol Bioeng. 2003;81(7):800-08.

36. Kellam B, De Bank PA, Shakesheff KM. Chemical modification of mammalian cell surfaces. Chem Soc Rev. 2003;32(6):327-37.

37. Peng L, Calton GJ, Burnett JW. Effect of borohydride reduction on antibodies. Appl Biochem Biotechnol. 1987;14(2):91-99.

38. Yang H, Lopina S, DiPersio L, Schmidt S. Stealth dendrimers for drug delivery: correlation between PEGylation, cytocompatibility, and drug payload. J Mater Sci. 2008;19(5):1991-97.

39. Yang H, Lopina ST. Penicillin V-conjugated PEG-PAMAM star polymers. J Biomater Sci Polym Ed. 2003;14(10):1043-56.

40. Diebold Y, Jarrin M, Saez V, Carvalho EL, Orea M, Calonge M, et al. Ocular drug delivery by liposome-chitosan nanoparticle complexes. Biomaterials. 2007;28(8):1553-64.

41. Lele BS, Hoffman AS. Insoluble ionic complexes of polyacrylic acid with a cationic drug for use as a mucoadhesive, ophthalmic drug delivery system. J Biomater Sci Polym Ed. 2000 Jan;11(12):1319-31.

42. Rozier A, Maznel C, Grove J, Plazonnet B. Gelrite®: a novel, ion activated, in situ gelling polymer for ophthalmic vehicles. Effect on bioavailability of timolol. Int J Pharm. 1989;57(2):163-8.

43. Balasubramaniam J, Pandit JK. Ion-activated in situ gelling systems for sustained ophthalmic delivery of ciprofloxacin hydrochloride. Drug Deliv. 2003;10(3):185-91.

44. Jain SP, Shah SP, Rajadhyaksha NS, Singh PSP, Amin PD. In situ ophthalmic gel of ciprofloxacin hydrochloride for once a day sustained delivery. Drug Dev Ind Pharm. 2008;34(4):445-52.

45. Mansour M, Mansour S, Mortada ND, Elhady SS. Ocular poloxamer-based ciprofloxacin hydrochloride in situ forming gels. Drug Dev Ind Pharm. 2008 Jul;34(7):744-52.

46. Gratieri T, Gelfuso GM, Rocha EM, Sarmento VH, de Freitas O, Lopez RF. A poloxamer/chitosan in situ forming gel with prolonged retention time for ocular delivery. Eur J Pharm Biopharm. 2010 Jun;75(2):186-93.

47. Cortesi R, Argnani R, Esposito E, Dalpiaz A, Scatturin A, Bortolotti F, et al. Cationic liposomes as potential carriers for ocular administration of peptides with anti-herpetic activity. Int J Pharm. 2006 Jul;317(1):90-100.

48. Zimmer A, Mutschler E, Lambrecht G, Mayer D, Kreuter J. Pharmacokinetic and pharmacodynamic aspects of an ophthalmic pilocarpine nanoparticle-delivery-system. Pharm Res. 1994 Oct;11(10):1435-42.

49. Ibrahim HK, El-Leithy IS, Makky AA. Mucoadhesive nanoparticles as carrier systems for prolonged ocular delivery of gatifloxacin/prednisolone bitherapy. Mol Pharm. 2010 Feb;7(2):576-85.

50. Amrite AC, Kompella UB. Size-dependent disposition of nanoparticles and microparticles following subconjunctival administration. J Pharm Pharmacol;2005 Dec;57(12):1555-63.

51. Kang S, Durairaj C, Kompella U, O'Brien J, Grossniklaus H. Subconjunctival nanoparticle carboplatin in the treatment of murine retinoblastoma. Arch Ophthalmol. 2009 Aug;127(8):1043-47.

52. Tomalia DA, Baker H, Dewald J, Hall M, Kallos G, Martin S, et al. A new class of polymers: starburst-dendritic macromolecules. Polym J. 1985;17(1):117-32.

53. Carnahan MA, Middleton C, Kim J, Kim T, Grinstaff MW. Hybrid dendritic-linear polyester-ethers for in situ photopolymerization. J Am Chem Soc. 2002 May;124(19):5291-3.

54. Degoricija L, Johnson CS, Wathier M, Kim T, Grinstaff MW. Photo cross-linkable biodendrimers as ophthalmic adhesives for central lacerations and penetrating keratoplasties. Invest Ophthalmol Vis Sci. 2007 May;48(5):2037-42.

55. Velazquez AJ, Carnahan MA, Kristinsson J, Stinnett S, Grinstaff MW, Kim T. New dendritic adhesives for sutureless ophthalmic surgical procedures: in vitro studies of corneal laceration repair. Arch Ophthalmol. 2004 Jun;122(6):867-70.

56. Yang H, Morris JJ, Lopina ST. Polyethylene glycol-polyamidoamine dendritic micelle as solubility enhancer and the effect of the length of polyethylene glycol arms on the solubility of pyrene in water. J Colloid Interface Sci. 2004;273(1):148-54.

57. Takeuchi H, Thongborisute J, Matsui Y, Sugihara H, Yamamoto H, Kawashima Y. Novel mucoadhesion tests for polymers and polymer-coated particles to design optimal mucoadhesive drug delivery systems. Adv Drug Deliv Rev. 2005 Nov;57(11):1583-94.

58. Bhagav P, Deshpande P, Pandey S, Chandran S. Development and validation of stability indicating UV spectrophotometric method for the estimation of brimonidine tartrate in pure form, formulations and preformulation studies. Der Pharmacia Lettre. 2010;2(3):106-22.

59. Kompella UB, Sundaram S, Raghava S, Escobar ER. Luteinizing hormone-releasing hormone agonist and transferrin functionalizations enhance nanoparticle delivery in a novel bovine ex vivo eye model. Mol Vis. 2006 Oct;12:1185-98.

60. Kitchens K, Kolhatkar M, Swaan R, Eddington B, Ghandehari P. Transport of poly(amidoamine) dendrimers across caco-2 cell monolayers: influence of size, charge and fluorescent labeling. Pharm Res. 2006 Dec;23(12):2818-26.

61. Gahmberg CG, Tolvanen M. Nonmetabolic radiolabeling and tagging of glycoconjugates. Meth Enzymol. 1994;230:32-44.

62. Mahal LK, Yarema KJ, Bertozzi CR. Engineering chemical reactivity on cell surfaces through oligosaccharide biosynthesis. Science. 1997 May;276(5315):1125-28.

63. Premkumar DR, Fukuoka Y, Sevlever D. Properties of exogenously added GPI-anchored proteins following their incorporation into cells. J Cell Biochem. 2001 Aug;82(2):234-45.

64. Hussey SL, He E, Peterson BR. A synthetic membrane-anchored antigen efficiently promotes uptake of antifluorescein antibodies and associated protein a by mammalian cells. J Am Chem Soc. 2001 Dec;123(50):12712-13.

65. Gupta SK, Agarwal R, Galpalli ND. Comparative efficacy of pilocarpine, timolol and latanoprost in experimental models of glaucoma. Methods Find Exp Clin Pharmacol. 2007 Dec;29(10):665-671.

66. Keppler OT, Stehling P, Herrmann M. Biosynthetic modulation of sialic acid-dependent virus-receptor interactions of two primate polyoma viruses. J Biol Chem. 1995 Jan;270(3):1308-14.

67. Burchenal JE, Deible CR, Deglau TE. Polyethylene glycol diisocyanate decreases platelet deposition after balloon injury of rabbit femoral arteries. J Thromb Thrombolysis. 2002 Feb;13(1):27-33.

68. Panza JL, Wagner WR, Rilo HL. Treatment of rat pancreatic islets with reactive PEG. Biomaterials. 2000 Jun;21(11):1155-64.

69. Lemieux GA, Bertozzi CR. Chemoselective ligation reactions with proteins, oligosaccharides and cells. Trends Biotechnol. 1998 Dec;16(12):506-13.

70. Choi YS, Hong SR, Lee YM. Studies on gelatin-containing artificial skin: II. Preparation and characterization of crosslinked gelatin-hyaluronate sponge. J Biomed Mater Res. 1999 Sep;48(5):631-639.

71. Martin SE, Peterson BR. Non-natural cell surface receptors: synthetic peptides capped with N-cholesterylglycine efficiently deliver proteins into mammalian cells. Bioconjug Chem. 2003 Nov;14(1):67-74.

72. Liu T, Guo Z, Yang Q, Sad S, Jennings HJ. Biochemical engineering of surface alpha 2-8 polysialic acid for immunotargeting tumor cells. J Biol Chem. 2000 Oct;275(42):32832-36.

73. Ong SM, He L, Thuy-Linh NT. Transient inter-cellular polymeric linker. Biomaterials. 2007 Sep;28(25):3656-67.

74. Paul S, Snary D, Hoebeke J, Allen D, Balloul JM, Bizouarne N, et al. Targeted macrophage cytotoxicity using a nonreplicative live vector expressing a tumor-specific single-chain variable region fragment. Hum Gene Ther. 2000 Jul;11(10):1417-28.

75. Choi M, Stanton-Maxey K, Stanley J, Levin C, Bardhan R, Akin D, et al. A cellular Trojan Horse for delivery of therapeutic nanoparticles into tumors. Nano Letters. 2007 Dec;7(12):3759-65.

76. Howarth M, Takao K, Hayashi Y, Ting A. Targeting quantum dots to surface proteins in living cells with biotin ligase. Proc Nat Acad of Sci. 2005 May;102(21):7583-88.

77. Roberts JC, Bhalgat MK, Zera RT. Preliminary biological evaluation of polyamidoamine (PAMAM) starburst dendrimers. J Biomed Mater Res. 1996 Jan;30(1):53-65.

78. Xyloyannis M, Padilla De Jesus OL, Frechet JMJ, Duncan R. PEG-dendron architecture influences endocytic capture and intercellular trafficking. Proc Int Symp Controlled Release Bioact Mater. 2003;30:149.

79. Kailasan A, Yuan Q, Yang H. Synthesis and characterization of thermoresponsive polyamidoamine–polyethylene glycol–poly(d, l-lactide) core–shell nanoparticles. Acta Biomaterialia. 2010 Mar;6(3):1131-39.

80. Yang H, Lopina S. In vitro enzymatic stability of dendritic peptides. J Biomed Mat Research. 2006 Feb;76(2):398-407.

81. Templeton AC, Cliffel DE, Murray RW. Redox and fluorophore functionalization of water-soluble, tioprenin-protected gold clusters. J Am Chem Soc. 1999;121(30):7081-89.

82. Hornsey VS, Prowse CV, Pepper DS. Reductive amination for solid-phase coupling of protein. A practical alternative to cyanogen bromide. J Immunol Methods. 1986 Oct;93(1):83-88.

83. Yang H, Kao JW. Synthesis and characterization of nanoscale dendritic RGD clusters for potential applications in tissue engineering and drug delivery. Int J Nanomedicine. 2007;2(1):89-99.

84. Yang H, Lopina ST. Extended release of a novel antidepressant, venlafaxine, based on anionic polyamidoamine dendrimers and poly(ethylene glycol)-containing semi-interpenetrating networks. J Biomed Mater Res. 2005 Jan;72(1):107-14.

85. Yang H, Tyagi P, Kadam RS, Holden CA, Kompella UB. Hybrid dendrimer hydrogel/PLGA nanoparticle platform sustains drug delivery for one week and antiglaucoma effects for four days following one-time topical administration. ACS Nano. 2012 Aug;6(9):7595-7606.

86. Lancina III MG, Singh S, Kompella UB, Husain S, Yang H. Fast dissolving dendrimer nanofiber mats as alternative to eye drops for more efficient antiglaucoma drug delivery. ACS Biomat Sci Eng. 2017 Jun.

87. Xu L, Cooper RC, Wang J, Yeudall WA, Yang H. Synthesis and application of injectable bioorthogonal dendrimer hydrogels for local drug delivery. ACS Biomat Sci Eng. 2017 Jun.

Vita

Christopher Alan Holden was born on September 7, 1984, in Morganton, NC. He graduated from Fauquier High School in Warrenton, VA in 2003 and subsequently graduated from the University of Virginia with a B.S. in Biomedical Engineering in 2007. In his second year at VCU, Chris joined the Yang lab for Biomaterials and Drug Delivery and started his work researching dendrimer biomaterials. Chris published two first author journal articles and presented his works at two national Society for Biomaterials conferences. Chris was also involved in extracurricular activities as co-founder and president of the student chapter of Engineers Without Borders at VCU. The EWB-VCU chapter raised funding for and visited Bolivia for a water quality assessment trip under his leadership. Chris and his brother, Andrew, are co-owners of an upscale American restaurant called Cedar Knoll near the historic Mt Vernon in Alexandria. Chris graduated with his Masters in Biomedical Engineering from VCU in August of 2017. He hopes to find work in the future as a science liaison or in science policy.